European Journal of Medicinal Chemistry 308 (2026) 118716

Contents lists available at ScienceDirect

European Journal of Medicinal Chemistry

journal homepage: www.elsevier.com/locate/ejmech

Research paper

Steroidal hormones and neurosteroids - novel therapeutic strategies in bacterial infections: Design, synthesis, and biological evaluation

Daniela Brdová [a], Bára Křížkovská [a], Jan Špaček [a], Zdeněk Míchal [a], Eva Jablonská [a], Ondřej Strnad [a], Hana Chodounská [b], Eszter Szánti-Pintér [b], Marina Morozovová [b], Václav Hanžl [a], Jan Tkadlec [c], Martijn Riool [d], Jan Lipov [a], Jitka Viktorová [a,*], Eva Kudová [b,**]

[a] Department of Biochemistry and Microbiology, University of Chemistry and Technology Prague, Technická 5, Prague, 166 28, Czech Republic
[b] Institute of Organic Chemistry and Biochemistry of the Czech Academy of Sciences, Flemingovo náměstí 2, Prague 6, 166 10, Czech Republic
[c] Department of Medical Microbiology, Charles University, 2nd Faculty of Medicine and Motol University Hospital, V Úvalu 84, Prague 5, 150 06, Czech Republic
[d] Department of Trauma Surgery, University Hospital Regensburg, Franz-Josef-Straußβ-Allee 11, Regensburg, 93053, Germany

ARTICLE INFO

Keywords:
Steroid hormones
Neurosteroids
Androstane
Efflux pump inhibition
Staphylococcus aureus
Adjuvant therapy

ABSTRACT

The global rise of antibiotic resistance necessitates novel therapeutic strategies for infectious diseases. Inhibition of bacterial efflux pumps, which contribute to multidrug resistance, represents a promising approach to restore or even increase the efficacy of existing antibiotics. Using fluorescence-based ethidium bromide accumulation, broth microdilution, and checkerboard assays, we evaluated 26 endogenous steroidal hormones and neurosteroids, along with 30 synthetic derivatives, for their ability to enhance antibiotic susceptibility in multidrug-resistant *Staphylococcus aureus*. Structure-activity relationship analysis identified compounds **13** and **16** as lead candidates, exhibiting strong efflux pump inhibition and marked reductions in the minimum inhibitory concentrations of ciprofloxacin and erythromycin. Both compounds showed additive effects in checkerboard assays. Modifications at C-3 (polar substitution) and C-17 (3α,5β-stereochemistry and nonpolar substitution) were essential for potent efflux inhibition and sensitization, although these modifications were not additive when combined. Transcriptome analysis further revealed that compound **13** significantly downregulated *S. aureus* virulence-associated genes when administered alone or in combination with antibiotics. Cytotoxicity assessment in human peripheral blood mononuclear cells and receptor transactivation assays for estrogen, androgen, and progesterone receptors indicated that the most active derivatives were non-toxic and lacked detectable endocrine activity, suggesting a favorable safety profile. Overall, these findings support the concept that rationally designed andostane-based steroidal scaffolds can function as competitive bacterial efflux pump inhibitors and serve as potential antibiotic adjuvants to mitigate efflux-mediated resistance.

1. Introduction

Steroid hormones are a class of biologically active molecules derived from cholesterol that play crucial regulatory roles in the human body [1]. These lipophilic compounds are synthesized primarily in the adrenal glands, gonads, and central nervous system through a series of enzyme-mediated reactions [2]. Steroid hormones exert *genomic effects* by binding to intracellular nuclear receptors [3], which act as ligand-activated transcription factors to regulate gene expression within target cells. This leads to long-term changes in protein synthesis and cellular function, such as altered metabolism or growth. The complex biochemical pathways of steroidogenesis involve multiple physiologically relevant molecules, as illustrated in Fig. 1. Based on their structural features and physiological functions, steroid hormones are commonly classified into four main categories: progestogens, androgens, estrogens, and corticosteroids (including glucocorticoids and mineralocorticoids). A distinct group of steroids is neurosteroids [4], endogenous compounds synthesized within the brain and nervous system from cholesterol or circulating steroid precursors. Neurosteroids and their synthetic analogues (neuroactive steroids) rapidly modulate neuronal excitability by interacting with neurotransmitter receptors such as γ-aminobutyric acid A ($GABA_A$), *N*-methyl-D-aspartate (NMDA), or G-protein coupled

* Corresponding author.
** Corresponding author.
E-mail addresses: prokesoj@vscht.cz (J. Viktorová), eva.kudova@uochb.cas.cz (E. Kudová).

https://doi.org/10.1016/j.ejmech.2026.118716
Received 2 December 2025; Received in revised form 18 February 2026; Accepted 20 February 2026
Available online 21 February 2026

receptors. As neurosteroids do not target nuclear receptors, their mechanism of action is defined as *non-genomic*.

The classification of "steroid hormones and neurosteroids" reflects not only chemical structure but also distinct biological activities, ranging from the modulation of immune responses and metabolic homeostasis to the regulation of neurobiological processes [5]. Physiological concentrations of steroid hormones can range from picomolar levels, such as estrogens and progesterone [6], to nanomolar levels, as seen in corticosteroids like cortisol [7]. Some hormones, including dehydroepiandrosterone (DHEA) and testosterone, can reach micromolar concentrations, especially in certain tissues [8]. It should also be noted that steroid hormones and neurosteroids undergo profound changes in their concentrations and physiological roles throughout pregnancy [9–11]. In pathological conditions, hormone levels can be significantly altered; for instance, cortisol levels may exceed micromolar concentrations in Cushing's syndrome [12], severe stress or sepsis [13], while estrogens, DHEA, or testosterone can also be elevated or suppressed in various endocrine disorders [14], highlighting their potent biological effects across a wide concentration range.

Recently, significant attention has been paid to steroids for their potential therapeutic value, not only in neurology and psychiatry, but also in modulating immune function and susceptibility to infectious diseases [15]. Many studies have demonstrated the ability of microorganisms to respond to host signaling molecules, including steroid hormones. These hormones interact with bacteria in a complex manner, influencing various aspects of bacterial behavior, including growth, antimicrobial susceptibility, metabolism, stress responses, quorum sensing, and virulence [16–18]. Moreover, recent research has highlighted the role of steroids in personalized medicine, considering gender and hormonal status as key factors in therapeutic strategies. Studies have shown that sex steroid hormones impact bacterial-host interactions and infection susceptibility in a sex-specific manner [19,20]. Additionally, it has been shown that androgens and glucocorticoids affect microbial growth and antibiotic resistance, underscoring the significance of steroid hormones in microbial behavior and antimicrobial susceptibility [21].

Bacterial resistance to antibiotics is a major concern in modern medicine, and one of the fundamental mechanisms of bacterial resistance is the overproduction of efflux pumps, which actively transport antibiotics from the intracellular to the extracellular space, thereby reducing their intracellular concentration below the therapeutic threshold and rendering the antibiotics less effective [22]. Efflux pumps are essential for bacterial survival, as they help eliminate toxic compounds, including both endogenous metabolites and foreign substances like antibiotics.

Human cells also employ efflux pumps to maintain hormonal balance and cellular homeostasis, and they are essential for the active transport of endogenous steroid hormones across biological membranes. This transport is critical not only for the clearance of excess steroids from cells but also for shaping hormone gradients between tissues, controlling local hormone availability, and terminating hormone signaling after receptor activation. Several well-characterized human efflux pumps, particularly those from the ATP-binding cassette (ABC) transporter family, such as P-glycoprotein (MDR1/ABCB1), breast cancer resistance protein (BCRP/ABCG2), and multidrug resistance (MDR)-associated proteins, are known to mediate the export of steroid hormones and their metabolites [23].

Interestingly, several of these human transporters share structural and functional similarity with bacterial efflux pumps, such as those from the resistance-nodulation-division (RND) and ABC families. This similarity raises the intriguing possibility that bacterial efflux systems may also interact with steroid molecules, which could also serve as substrates for bacterial efflux systems [24,25]. Bacteria, such as *Staphylococcus aureus*, adapt to environmental stress, including exposure to antibiotics, by increasing the production of efflux pumps that actively expel antimicrobial agents. One of the well-characterized examples is the NorA efflux pump, a member of the major facilitator superfamily (MFS), which helps the bacteria resist a broad spectrum of compounds, including fluoroquinolones [22].

Given that human steroid hormones are known substrates for various human efflux pumps, it is conceivable that structurally similar molecules may interact with bacterial efflux systems as well. In this context, steroid hormones could act as competitive inhibitors of bacterial efflux pumps, binding to the transporter and effectively competing with antibiotics for export. This interaction could reduce antibotic efflux, thereby increasing their intracellular concentration and potentially enhancing antibacterial efficacy. The goal of this study was to investigate this hypothesis further and evaluate whether structural modification of endogenous steroids can yield more effective inhibitors of bacterial efflux pumps. If successful, this strategy could represent a novel adjuvant therapy.

2. Materials and methods

2.1. Chemistry

2.1.1. General

All commercial reagents and solvents were used without further purification. Melting points were determined with a micromelting point

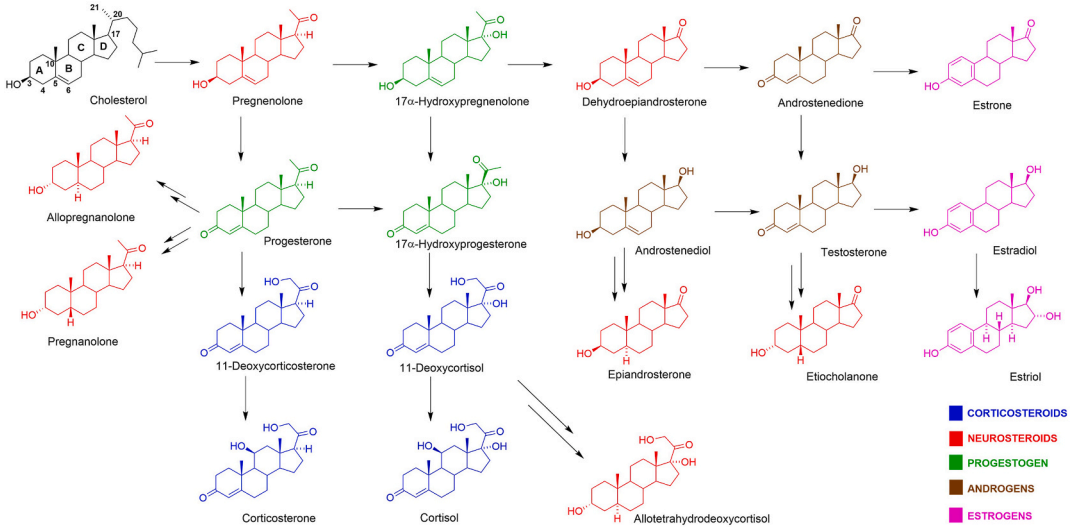

Fig. 1. Overview of steroidal hormones and endogenous neurosteroids tested in the primary screening.

apparatus (Helmut Hund, Germany) and are uncorrected. For elemental analysis, a PE 2400 Series II CHNS/O Analyzer (PerkinElmer, MA, USA) was used, with a microbalance MX5 (Mettler Toledo, Switzerland). Optical rotation were measured on a AUTOPOL IV polarimeter (Rudolph Research Analytical, NJ, USA); all samples were measured at 20 °C, at the specified concentration in the indicated solvent at 589 nm. Proton and carbon NMR spectra were recorded on a AVANCE III 400 MHz (Bruker, Germany) spectrometer, with chemical shifts given in parts per million (ppm δ), relative to the residual $CDCl_3$ peak at 7.26 and 77.16 ppm for ^1H and ^{13}C nuclei, respectively. Coupling constants (J) are reported in Hz. The high resolution mass spectrometry (HRMS) spectra were obtained on an LTQ Orbitrap XL (Thermo Fisher Scientific, MA, USA) in electrospray ionization (ESI) mode. Thin-layer chromatography (TLC) was performed on silica gel plates (Merck, Czech Republic, 60 μm) and visualized with a phosphomolybdic acid/ethanol stain. For flash chromatography, the puriFlash 5.250 system (Interchim, France) was used, with neutral silica gel (Merck, 40–63 μm) and an evaporative light scattering detector (ELSD) detector. Analytical samples were dried over phosphorus pentoxide at 25 °C and 0.25 kPa.

2.1.2. Synthesis

2.1.2.1. Library of endogenous steroidal hormones and neurosteroids (Fig. 1). All compounds listed below were obtained from the internal Library of Steroidal Compounds maintained at Institute of Organic Chemistry and Biochemistry (IOCB Prague). Each was originally purchased from the indicated commercial supplier.

Pregnenolone (3β-Hydroxy-pregn-5-en-20-one), Merck, CAS 145-13-1, Cat. No. PHR2564.

17α-Hydroxypregnenolone (3β,17α-Dihydroxy-pregn-5-en-20-one), Biosynth Ltd., United Kingdom, CAS 387-79-1, Cat. No. FH40258.

Dehydroepiandrosterone (3β-Hydroxy-androst-5-en-17-one), Merck, CAS 53-43-0, Cat. No. 700087P.

Androstenedione (Androst-4-ene-3,17-dione), Merck, CAS 63-05-8, Cat. No. 46033.

Estrone (3-Hydroxyestra-1,3,5(10)-trien-17-one), LGC Ltd., United Kingdom, CAS 53-16-7, Cat. No. TRC-E889050.

Progesterone (Pregn-4-ene-3,20-dione), Merck, CAS 57-83-0, Cat. No. P8783.

Allopregnanolone (3α-Hydroxy-5α-pregnan-20-one). Biosynth Ltd., CAS 516-54-1, Cat. No. FA158661.

Pregnanolone (3α-Hydroxy-5β-pregnan-20-one), Tocris, Bio-Techne R&D Systems, Czech Republic, CAS 128-20-1, Cat. No. 3652.

17α-Hydroxyprogesterone (17α-Hydroxy-pregn-4-ene-3,20-dione), Merck, CAS 68-96-2, Cat. No. H5752.

Androstenediol (Androst-5-ene-3β,17β-diol), LGC Ltd., CAS 521-17-5, Cat. No. TRC-A637670.

Testosterone (17β-Hydroxyandrost-4-en-3-one), Merck, CAS 58-22-0, Cat. No. PHR2027.

Estradiol (Estra-1,3,5(10)-triene-3,17β-diol), Merck, CAS 50-28-2, Cat. No. E8875.

11-Deoxycorticosterone (21-Hydroxypregn-4-ene-3,20-dione), Merck, CAS 64-85-7, Cat. No. D6875.

11-Deoxycortisol (17α,21-Dihydroxypregn-4-ene-3,20-dione), Merck, CAS 152-58-9, Cat. No. R0500.

Epiandrosterone (3β-Hydroxy-5α-androstan-17-one), Merck, CAS 481-29-8, Cat. No. E3375.

Etiocholanolone (3α-Hydroxy-5β-androstan-17-one), Merck, CAS 53-42-9, Cat. No. E5126.

Estriol (Estra-1,3,5(10)-triene-3,16α,17β-triol), Merck, CAS 50-27-1, Cat. No. PHR2800.

Corticosterone (11β,21-Dihydroxypregn-4-ene-3,20-dione), Merck, CAS 50-22-6, Cat. No. 27840.

Cortisol (11β,17α,21-Trihydroxypregn-4-ene-3,20-dione), Merck, CAS 50-23-7, Cat. No. H4001.

Allotetrahydrodeoxycortisol (3α,17α,21-Trihydroxy-5α-pregnan-20-one), Biosynth Ltd., CAS 601-01-4, Cat. No. FA65668.

2.1.2.2. Library of C-3, C-5, and C-20 reduced metabolites of progesterone (Fig. 2). All compounds listed below were obtained from the internal Library of Steroidal Compounds maintained at IOCB Prague. Each was originally purchased from the indicated commercial supplier.

(20S)-Hydroxyprogesterone (20α-Hydroxypregn-4-en-3-one), Santa Cruz Biotechnology, Inc., United States, CAS 145-14-2, Cat. No. sc-396005.

(3β)-Hydroxyprogesterone (3β-Hydroxy-pregn-4-ene-20-one), LGC Ltd., CAS 566-66-5, Cat. No. TRC-H939040.

5α-Pregnane-3,20-dione (5α-Dihydroprogesterone), Biosynth Ltd., CAS 566-65-4, Cat. No. FP40764.

5β-Pregnane-3,20-dione (5β-Dihydroprogesterone), LGC Ltd., CAS 566-66-5, Cat. No. D449280.

Isopregnanolone (3β-Hydroxy-5α-pregnan-20-one), LGC Ltd., CAS 516-55-2, Cat. No. TRC-I822200.

Epipregnanolone (3β-Hydroxy-5β-pregnan-20-one), Biosynth Ltd., CAS 128-21-2, Cat. No. FE177267.

*2.1.2.3. Compounds 1–33. 20-Oxo-5β-pregnan-3α-yl 3-Hemisuccinate (**1**).* Compound **1** was prepared according to the literature [26].

*3α-Amino-5β-pregnan-20-one hydrochloride (**2**).* Compound **2** was prepared according to the literature [27].

*20-Oxo-5β-pregnan-3α-yl L-Glutamyl 1-Ester (**3**).* Compound **3** was prepared according to the literature [28].

(3R,5R,8R,9S,10S,13S,14S,17S)-17-acetyl-10,13-dimethylhexadecahydro-1H-cyclopenta[a]phenanthren-3-yl *(S)-5-oxopyrrolidine-2-carboxylate (**4**).* Compound **4** was prepared according to the literature [29].

*17α-Oxo-D-homo-5β-androstan-3α-ol (**5**).* Compound **5** was prepared according to the literature [30].

*17-Methylene-5β-androstan-3α-ol (**6**).* Compound **6** was prepared according to the literature [30].

*3α-Hydroxy-5β-androstane (**7**).* Compound **7** was prepared according to the literature [30].

*3α-Hydroxy-17β-methyl-5β-androstane (**8**).* Compound **8** was prepared according to the literature [30].

Compounds **9**, **11** and **12** listed below were obtained from the internal Library of Steroidal Compounds maintained at IOCB Prague. Each was originally purchased from the indicated commercial supplier.

*17α-Hydroxypregnanolone (3α,17α-Dihydroxy-5β-pregnan-20-one, **9**),* Alfa Chemistry, USA, CAS 570-52-5, Cat. No. ACM570525.

*11α-Hydroxypregnanolone (3α,11α-Dihydroxy-5β-pregnan-20-one, **10**).* Compound **10** was prepared according to the literature [31].

*Tetrahydrocorticosterone (3α,11β,21-Trihydroxy-5β-pregnan-20-one, **11**).* LGC Ltd., CAS 68-42-8, Cat. No. TRC-T293160.

*11,20-Dioxo-5β-pregnane-3α,21-diol (**12**).* Biosynth Ltd., CAS 128-21-2, Cat. No. FE177267.

2-(((3R,5R,8S,9S,10S,13S,14S)-10,13-dimethylhexadecahydro-1H-cyclopenta[a]phenanthren-3-yl*)oxy)ethan-1-ol (**13**).* Lithium aluminum hydride (265 mg, 7.05 mmol) was added to a solution of carboxylic acid **32** (1.7 g, 5.1 mmol) in tetrahydrofuran (THF, d60 mL). The reaction mixture was refluxed for 2 h. Then, the reaction was quenched by adding a small amount of saturated aqueous sodium sulfate at 0 °C, and the resulting precipitated solid material was filtered off. The filtrate was extracted with ethyl acetate (3 × 20 mL). The combined organic layers were washed with water and brine, dried over Na_2SO_4. Solvents were evaporated *in vacuo*. Crystallization afforded compound **13** (1.4 g, 93%): mp 160–162 °C (EtOAc/*n*-heptane), $[\alpha]_D^{20}$ +12.4 (*c* 0.2, $CHCl_3$). ^1H NMR (400 MHz, chloroform $CDCl_3$): δ 0.68 (s, 3H-18), 0.93 (s, 3H-19), 3.30 (m, H-3), 3.59 (ddd, J = 6.1, 3.5, 1.2 Hz, 2H, C-1′), 3.72 (m, 2H, C-2′). ^{13}C NMR (101 MHz, $CDCl_3$): δ 79.8 (C-3), 69.0 (C-2′), 62.3 (C-1′), 54.7, 42.3, 41.1, 40.8, 40.6, 39.2, 36.4, 35.6, 35.2, 33.4, 27.5, 27.4, 26.9,

25.7, 23.6, 21.0, 20.7, 17.6. IR spectrum ($CHCl_3$): 3630, 3595 (OH); 2935, 2867 (CH_2); 1052 (C–OH). MS (ESI) *m/z*: 343.3 (100%, M + Na). HR-MS (ESI) *m/z* for $C_{21}H_{36}O_2Na$ [M+Na] calcd. 343.26075, found 343.26070.

*2-(Dimethylamino)-N-[(17β-methyl-5β-androstan-3α-yl] Acetamide **(14)***. 3α-Amino-17β-methyl-5β-androstan hydrochloride [32] (325.9 mg, 1 mmol) and 4-(*N*,*N*-dimethylamino)pyridine (122.2 mg, 1 mmol) were placed in a round-bottom flask equipped with a septum inlet, then it was evacuated and refilled with argon two times. The solids were dissolved in 20 mL dichloromethane (DCM) and upon stirring, *N*,*N*-diisopropylethylamine (609 μL, 3.5 mmol) was added. It was followed by the addition of 1-ethyl-3-(3-dimethylaminopropyl)carbodiimide hydrochloride (EDCI, 479 mg, 2.5 mmol) and *N*,*N*-dimethylglycine (258 mg, 2.5 mmol, 2.5 eq.) under an argon stream. The reaction mixture was stirred at room temperature for 24 h. The solvent was evaporated, and the crude mixture was dissolved in 70 mL DCM. It was washed twice with 15 mL of water, then the organic phase was dried over anhydrous sodium sulfate. It was filtered, and the solvent evaporated. Chromatography on silica gel (1–3% acetone in chloroform) gave compound **14** (311 mg, 83%) as a white solid: mp 141–143 °C (chloroform/acetone); $[\alpha]_D^{20}$ +44.9 (*c* 0.254, $CHCl_3$). ^{1}H NMR (400 MHz, $CDCl_3$): δ 0.53 (3H, s, H-18), 0.83 (3H, d, $J = 6.8$ Hz, H-17), 0.95 (3H, s, H-19), 2.30 (6H, s, $N(CH_3)_2$), 2.93 (2H, s, N–CH_2–CO), 3.81 (1H, m, H-3), 7.00 (1H, d, $J = 6.3$ Hz, NH). ^{13}C NMR (101 MHz, $CDCl_3$): δ 169.5 (CO–NH), 63.4 (N–CH_2–CO), 56.1, 48.8, 46.0, 45.4, 42.7, 42.4, 41.1, 37.9, 36.2, 36.2, 34.9, 33.9, 30.4, 28.2, 27.2, 26.8, 24.9, 23.8, 20.7, 14.0, 12.2. IR spectrum ($CHCl_3$): 3355 (NH), 1660 (amide I), 1522 (amide II), 1046 (N–C_3). MS (ESI) *m/z*: 375.3 (100 %, M + H). HRMS (ESI) *m/z* for $C_{24}H_{43}N_2O$ [M+H] calcd. 375.33699, found 375.33694. For $C_{24}H_{43}N_2O$ (374.3) calcd: 76.95 % C, 11.30 % H, 7.48 % N; found: 76.79 % C, 11.11 % H, 7.32 % N.

(3R,5R,8S,9S,10S,13S,14S)-10,13-Dimethylhexadecahydro-1H-cyclopenta[a]phenanthren-3-yl *(S)-5-oxopyrrolidine-2-carboxylate **(15)***. A mixture of compound **7** (300 mg, 1.0 mmol), 4-dimethylaminopyridine (30 mg, 0.25 mmol), EDCI (517 mg, 2.7 mmol), and hydroxybenzotriazole (HOBt, 297 mg, 2.2 mmol) was dried under vacuum at room temperature for 1 h. Then, dry dimethylformamide (DMF, 10 mL) was added under inert atmosphere, followed by the slow dropwise addition of L-pyroglutamic acid (190 mg, 1.9 mmol) in dry DMF (5 mL). The reaction mixture was allowed to stir overnight at room temperature. After solvent evaporation, the residue was purified by column chromatography on silica gel (5% acetone/chloroform), affording compound **15** (210 mg, 58%): mp 136−137 °C (chloroform/diethyl ether), $[\alpha]_D^{20}$ +29.5 (*c* 0.2, $CHCl_3$). ^{1}H NMR (400 MHz, $CDCl_3$): δ 0.69 (3H, s, H-18), 0.94 (3H, s, H-19), 4.18–4.53 (4H, m, pyroglutamic acid ester), 4.16-4.24 (1H, m, C-2′), 4.79 (1H tt, $J = 11.3$, 4.8 Hz, H-3), 5.89 (1H, s, N–H). ^{13}C NMR (101 MHz, $CDCl_3$): δ 177. 5 (CO–N), 171.4 (COO), 76.0 (C-3), 55.5, 54.5, 41.9, 40.9, 40.7, 40.5, 39.0, 36.2, 35.0, 34.7, 32.1, 29.2, 27.0, 26.7, 26.5, 25.5, 24.9, 23.3, 20.8, 20.6, 17.5. IR spectrum ($CHCl_3$): 1734, 1704 (C═O). MS ESI *m/z*: 386.3 (100%, M − H). HR-MS (ESI) *m/z* for $C_{24}H_{36}NO_3$ [M − H] calcd, 386.27007; found, 386.26962. For $C_{24}H_{37}NO_3$ (387.3) calcd: 74.38%, C; 9.62%, H; 3.61%N. Found: 74.20%, C; 9.61%, H; 3.26%, N.

4-(((3R,5R,8R,9S,10S,13S,14S)-10,13-Dimethyl-17-methylenhexadecahydro-1H-cyclopenta[a]phenantren-3-yl*)oxy)-4-oxobutanoic acid **(16)***. Compound **16** was prepared according to the literature [32].

3-(((3R,5R,8R,9S,10S,13S,14S)-10,13-Dimethyl-17-methylenehexadecahydro-1H-cyclo- penta[a]phenantren-3-yl*)oxy)-3-oxopropanoic acid **(17)***. Compound **17** was prepared according to the literature [32].

5-(((3R,5R,8R,9S,10S,13S,14S)-10,13-Dimethyl-17-methylenhexadecahydro-1H-cyclopenta[a]phenantren-3-yl*)oxy)-5-oxopentanoic acid **(18)***. Compound **18** was prepared according to the literature [32].

*20-Oxo-androst-5-en-3β-yl 3-Hemisuccinate **(19)***. Compound **19** was prepared according to the literature [33].

*17-Oxo-5β-androstan-3α-yl 3-Hemisuccinate **(20)***. Compound **20** was prepared according to the literature [32].

*20-Oxo-pregn-5-en-3β-yl 3-Hemisuccinate **(21)***. Compound **21** was prepared according to the literature [33,34].

*20-Oxo-5β-pregnan-3α-yl 3-Hemisuccinate **(22)***. Compound **22** was prepared according to the literature [26].

*20-Oxo-pregn-4-en-3β-yl 3-Hemisuccinate **(23)***. Compound **23** was prepared according to the literature [35].

3-(((3R,5R,8R,9S,10S,13S,17R)-10,13-dimethyl-17-(prop-1-en-2-yl*) hexadecahydro-1H-cyclopenta[a]phenanthren*-3-yl*)oxy)-3-oxopropanoic acid **(24)***. Compound **24** was prepared according to the literature [32].

4-(((3R,5R,8R,9S,10S,13S,14S,17R)-10,13-Dimethyl-17-(prop-1-en-2-yl*)hexadecahydro-1H-cyclopenta[a]phenantren*-3-yl*)oxy)-4-oxobutanoic acid **(25)***. Compound **25** was prepared according to the literature [32].

5-(((3R,5R,8R,9S,10S,13S,14S,Z)-17-Ethylidene-10,13-dimethylhexadecahydro-1H-cyclopenta[a]phenantren-3-yl*)oxy)-5-oxopentanoic acid **(26)***. Compound **26** was prepared according to the literature [32].

2-(((3R,5R,8S,9S,10S,13S,14S)-10,13-dimethylhexadecahydro-1H-cyclopenta[a]phenanthren-3-yl*)oxy)ethyl (R)-5-oxopyrrolidine-2-carboxylate **(27)***. A mixture of compound **13** (320 mg, 1.0 mmol), 4-dimethylaminopyridine (30 mg, 0.25 mmol), EDCI (517 mg, 2.7 mmol), and HOBt (297 mg, 2.2 mmol) was dried under vacuum at room temperature for 1 h. Then, dry DMF (10 mL) was added under inert atmosphere, followed by slow dropwise addition of L-pyroglutamic acid (194 mg, 1.5 mmol) in dry DMF (5 mL). The reaction mixture was allowed to stir overnight at room temperature. After solvent evaporation, the residue was purified by column chromatography on silica gel (5% acetone/hexane), affording compound **27** (180 mg, 42%): mp 110−111 °C (acetone/hexane), $[\alpha]_D^{20}$ +11.4 (*c* 0.30, $CHCl_3$). ^{1}HNMR (400 MHz, $CDCl_3$): δ 0.67 (3H, s, H-18), 0.92 (3H, s, H-19), 3.22–3.55 (m, 4H-lactam), 3.28 (m, H-3), 3.64–3.74 (2H, m, C1′), 4.28–4.30 (3H, m, 3H, C-2′ and C-4′), 5.92 (1H, s, lactam NH). ^{13}C NMR (101 MHz, $CDCl_3$): δ 177.6 (CO lactam), 172.1 (CO linker), 79.9 (C-3), 65.7, 65.3, 55.4, 54.7, 42.3, 41.1, 40.8, 40.6, 39.2, 36.3, 35.5, 35.3, 33.3, 29.2, 27.5, 27.2, 26.9, 25.7, 25.0, 23.6, 20.9, 20.7, 17.6. IR spectrum ($CHCl_3$): 3437, 1705 (oxopyrrolidine); 1744 (C═O); 1240, 1033 (C–O). MS ESI *m/z*: 454.3 (87%, M + Na), 432.3 (58%, M + H). HR-MS (ESI) *m/z* for $C_{26}H_{42}NO_4$ [M+H] calcd, 432.31084; found, 432.31049. For $C_{26}H_{41}NO_4$ (431.6) calcd: 72.35%, C; 9.58%, H; 3.25%, N. Found: 71.99%, C; 9.93%, H; 3.13%, N.

2-(((3R,5R,8S,9S,10S,13S,14S)-10,13-dimethylhexadecahydro-1H-cyclopenta[a]phenanthren-3-yl*)oxy)ethyl (S)-6-oxopiperidine-2-carboxylate **(28)***. A mixture of compound **13** (320 mg, 1.0 mmol), 4-dimethylaminopyridine (30 mg, 0.25 mmol), EDCI (517 mg, 2.7 mmol), and HOBt (297 mg, 2.2 mmol) was dried under vacuum at room temperature for 1 h. Then, dry DMF (10 mL) was added under inert atmosphere, followed by slow dropwise addition of (*S*)-6-oxo-2-piperidinecarboxylic acid (214 mg, 1.5 mmol) in dry DMF (5 mL). The reaction mixture was allowed to stir overnight at room temperature. After solvent evaporation, the residue was purified by column chromatography on silica gel (20% acetone/hexane), affording compound **27** (170 mg, 38%): mp 117−119 °C (acetone in hexane), $[\alpha]_D^{20}$ +8.1 (*c* 0.31, $CHCl_3$). ^{1}H NMR (400 MHz, $CDCl_3$): δ 0.67 (3H, s, H-18), 0.92 (3H, s, H-19), 2.16–2.24 (m, 1H, lactam), 2.30–2.44 (m, 2H, lactam), 3.27 (tt, $J = 11.1$, 4.6 Hz, H-3), 3.69 (ddd, $J = 5.5$, 4.2, 1.3 Hz, 2H, C-1′), 4.12 (ddd, $J = 8.3$, 5,1, 1,6 Hz, C-4′), 4.25–4.36 (m, 2H, C-2′), 6.11 (s, 1H, lactam NH). ^{13}C NMR (101 MHz, $CDCl_3$): δ 171.3 (CO lactam), 171.3 (CO linker), 79.9, 65.6, 65.4, 54.9, 54.7, 42.3, 41.1, 40.8, 40.6, 39.2, 36.3, 35.5, 35.2, 33.3, 31.2, 27.4, 27.2, 26.9, 25.7, 25.6, 23.6, 20.9, 20.7, 19.7, 17.6. IR spectrum ($CHCl_3$): 3400, 1666 (oxopiperidine); 1743 (C═O); 1294, 1244 (C–O). MS ESI *m/z*: 468.3 (100%, M + Na), 446.3 (88%, M + H). HR-MS (ESI) *m/z* for $C_{27}H_{44}NO_4$ [M+H] calcd, 446.32649; found, 446.32614. For $C_{27}H_{43}NO_4$ (445.6) calcd: 72.77%, C; 9.73%, H; 3.14%, N. Found: 72.63%, C; 9.65%, H; 3.03%, N.

(R)-N-(2-(((3R,5R,8S,9S,10S,13S,14S)-10,13-dimethylhexadecahydro-1H-cyclopenta[a]phenanthren-3-yl*)oxy)ethyl)-5-oxopyrrolidine-2-carboxamide **(29)***. The L-pyroglutamic acid (110 mg, 0.85 mmol) and 4-

dimethylaminopyridine (DMAP, 13.8 mg, 0.11 mmol) were dissolved in DCM (10 mL), and the resulting solution was cooled in an ice bath. EDCI (112 mg, 0.85 mmol) was added in one portion, and the mixture was stirred at 0 °C for 15 min. Steroid **33** (181 mg, 0.566 mmol) was then added in one portion, followed by *N*,*N*-diisopropylethylamine (DIPEA, 0.1 mL, 0.574 mmol). The solution was allowed to warm to room temperature and stirred overnight under an inert atmosphere. The reaction mixture was quenched with 5% HCl, extracted with chloroform (3 × 25 mL), washed with saturated aqueous solution of sodium bicarbonate (25 mL), dried over $MgSO_4$, and evaporated to dryness. The crude product was purified by flash column chromatography on silica gel (12 g, 0–10% ethanol in ethyl acetate), affording compound **29** (120 mg, 49%): mp 170-172 °C, $[\alpha]_D$ −8.9 (*c* 0.3 $CHCl_3$). ^{1}H NMR (401 MHz, $CDCl_3$): 0.68 (s, 3H-18), 0.92 (s, 3H-19), 2.11–2.60 (m, 4H-lactam), 3.26 (tt, J = 11.0, 4.6 Hz, H-3), 3.45 (m, 2H, C-2′), 3.54 (m, 2H, C-1′), 4.16 (ddd, J = 8.8, 5.1, 1.3 Hz, 1H, C-4′), 6.19 (s, 1H, lactam NH), 6.48 (s, 1H, linker NH). ^{13}C NMR (101 MHz, $CDCl_3$). δ 179.0 (CO lactam), 172.0 (CO linker), 79.9 (C-3), 66.3 (C-1′), 57.0, 54.7, 42.2, 41.1, 40.9, 40.6, 40.0, 39.2, 36.3, 35.5, 35.2, 33.3, 29.3, 27.4, 27.4, 26.9, 26.3, 25.7, 23.6, 21.0, 20.7, 17.6. IR spectrum ($CHCl_3$): 3430 (NH); 1704,1675 (CONH); 1096 (COC). MS (ESI) *m/z*: 453.3 (100%, M + Na). HR-MS (ESI) *m/z* for $C_{26}H_{42}O_3N_2Na$ [M+Na] calcd. 453.30876, found 453.30850.

*(S)–N-(2-(((3R,5R,8S,9S,10S,13S,14S)-10,13-dimethylhexadecahydro-1H-cyclopenta[a]phenanthren-*3-yl*)oxy)ethyl)-6-oxopiperidine-2-carboxamide (**30**)*. (*S*)-6-oxo-2-piperidinecarboxylic acid (122 mg, 0.85 mmol) and DMAP (13.8 mg, 0.11 mmol) were dissolved in DCM (10 mL), and the resulting solution was cooled in an ice bath. EDCI (112 mg, 0.85 mmol) was added in one portion, and the mixture was stirred at 0 °C for 15 min. Steroid **33** (181 mg, 0.566 mmol) was then added in one portion, followed by DIPEA (0.1 mL, 0.574 mmol). The solution was allowed to warm to room temperature and stirred for 46 h under an inert atmosphere. The reaction mixture was quenched with 5% HCl, extracted with chloroform (3 × 25 mL), washed with saturated aqueous solution of sodium bicarbonate (25 mL), dried over $MgSO_4$, and evaporated to dryness. The crude product was purified by flash column chromatography on silica gel (12 g, 0–10% ethanol in ethyl acetate), affording compound **30** (80 mg, 32%): mp 162–164 °C. ^{1}H NMR (401 MHz, $CDCl_3$): 0.67 (s, 3H-18), 0.91 (s, 3H-19), 2.39 (t, J = 6.7 Hz, 2H-lactam), 3.25 (tt, J = 11.0, 4.6 Hz, H-3), 3.45 (m, 2H, C-2′), 3.55 (m, 2H, C-1′), 4.02 (td, J = 5.9, 2.8 Hz, 1H, C-4′), 6.52 (s, 1H, linker NH), 6.73 (s, 1H, lactam NH). ^{13}C NMR (101 MHz, $CDCl_3$): δ 172.6 (CO lactam), 171.5 (CO linker), 79.8 (C-3), 66.3, 56.7, 54.6, 42.2, 41.0, 40.8, 40.6, 40.1, 40.0, 36.3, 35.5, 35.1, 33.2, 31.5, 27.4, 27.3, 26.9, 26.3, 25.7, 23.6, 20.9, 20.7, 18.9, 17.6. IR spectrum (CHCl3): 3434, 3392 (NH- amid, piperidine); 1664 (CONH); 1095 (COC). MS (ESI) *m/z*: 467.3 (100%, M + Na). HR-MS (ESI) *m/z* for $C_{27}H_{44}O_3N_2Na$ [M+Na] calcd. 467.32441, found 467.32455.

*Ethyl 2-(((3R,5R,8S,9S,10S,13S,14S)-10,13-dimethylhexadecahydro-1H-cyclopenta[a]phenanthren-*3-yl*)oxy)acetate (**31**)*. A solution of ethyl diazoacetate (1.62 mL, 15.4 mmol) in DCM (20 mL) was slowly added to a mixture of rhodium(II) acetate dimer (50 mg, 11.4 mmol) and compound **7** (1.38 g, 5 mmol) in DCM (100 mL). The reaction mixture was stirred under an argon atmosphere at room temperature for 2 h. The solvents were evaporated, and the crude product was purified by flash column chromatography on silica gel (80 g, 0–6% ethyl acetate in petroleum ether) to yield compound **31** (1.76 g, 97%) that was characterized by NMR spectroscopy and used directly in the next synthetic step. ^{1}H NMR (401 MHz, $CDCl_3$): δ 0.67 (s, 3H-18), 0.92 (s, 3H-19), 1.28 (t, J = 7.2 Hz, 3H, $OCH_2\underline{CH_3}$), 3.35 (m, H-3), 4.11 (s, 2H, C-1′), 4.22 (q, J = 7.1 Hz, 2H, $O\underline{CH_2}CH_3$). ^{13}C NMR (101 MHz, $CDCl_3$): δ 171.2 (COO), 80.3 (C-3), 65.9 (C-1′), 60.9 ($O\underline{CH_2}CH_3$), 54.7, 42.2, 41.1, 40.7, 40.6, 39.2, 36.3, 35.5, 35.1, 32.9, 27.4, 26.9, 26.9, 25.7, 23.5, 20.9, 20.7, 17.6, 14.4.

*2-(((3R,5R,8S,9S,10S,13S,14S)-10,13-dimethylhexadecahydro-1H-cyclopenta[a]phenanthren-*3-yl*)oxy)acetic acid (**32**)*. Potassium hydroxide (705 mg, 12.44 mmol) was added to a solution of ethyl ester **31** (1.76 g, 4.85 mmol) in EtOH (20 mL). The reaction mixture was stirred at 50 °C for 2 h, cooled, diluted with water (120 mL), and acidified to neutral pH. The product was extracted into DCM. The combined organic layers were washed with brine, dried over $MgSO_4$, and concentrated under reduced pressure. The crude product was purified by flash column chromatography on silica gel (40 g, 0–20% diethyl ether in petroleum ether with the addition of 1% of acetic acid) to yield compound **32** (1.41 g, 87%): mp 75–78 °C (diethyl ether), $[\alpha]_{20}$ +14.0 (*c* 0.2, $CHCl_3$). ^{1}H NMR (401 MHz, $CDCl_3$): δ 0.68 (s, 3H-18), 0.93 (s, 3H-19), 3.42 (m, 1H-3), 4.14 (s, 2H, C1′). ^{13}C NMR (101 MHz, $CDCl_3$): δ 172.9 (COO), 80.9 (C-3), 65.3 (C-1′), 54.7, 42.2, 41.1, 40.9, 40.6, 39.1, 36.3, 35.3, 35.1, 33.0, 27.3, 27.1, 26.9, 25.7, 23.5, 21.0, 20.7, 17.6. IR spectrum ($CHCl_3$): 3400 (OH); 1784, 1758 (C═O); 1120 (COC). MS (ESI) *m/z*: 333.2 (100%, M − 1). HR-MS (ESI) *m/z* for $C_{21}H_{33}O_3$ [M − 1] calcd. 333.24352, found 333.24329.

*2-(((3R,5R,8S,9S,10S,13S,14S)-10,13-dimethylhexadecahydro-1H-cyclopenta[a]phenanthren-*3-yl*)oxy)ethan-1-amine (**33**)*. A mixture of steroid alcohol **13** (2.022 g, 6.31 mmol), PPh_3 (1.884 g, 7.57 mmol), and phthalimide (1.056 g, 7.57 mmol) in dry THF (42 mL) was cooled to 0 °C and stirred for 1 h under an argon atmosphere. Then, diisopropyl azodicarboxylate (DIAD, 1.42 mL, 7.12 mmol) was added dropwise, and the reaction mixture was warmed overnight to room temperature while stirring. The solvents were partially evaporated, the reaction mixture was poured into brine, and the product was extracted with ethyl acetate (3 × 25 mL). The combined organic layers were washed with brine, dried over $MgSO_4$, and concentrated under reduced pressure. The crude C-3 phthalimide derivative was purified by flash column chromatography on silica gel (80 g, 0–10% ethyl acetate in petroleum ether). Next, C-3 phthalimide derivative (2.57 g, mmol) was dissolved in MeOH (30 mL), and hydrazine monohydrate (3 mL) was added. The mixture was refluxed for 2 h, cooled, and poured into brine. The crude product was extracted with ethyl acetate (3 × 20 mL), the combined organic layers were washed with brine, dried over Na_2SO_4, and the solvents were evaporated, yielding compound **33** (1.5 g, 74%): m.p. 167–168 °C, $[\alpha]_D$ −8.9 (*c* 0.3 $CHCl_3$). ^{1}H NMR (401 MHz, $CDCl_3$): 0.67 (s, 3H-18), 0.91 (s, 3H-19), 3.18 (m, 2H, C-2′), 3.36 (tt, J = 10.8, 4.3 Hz, H-3), 3.75 (t, J = 5.3 Hz, 2H, C-1′), 8.26 (s, 2H, NH_2). ^{13}C NMR (101 MHz, $CDCl_3$) δ 80.1 (C-3), 63.2 (C-1′), 54.6, 42.2, 41.1, 40.8, 40.6, 40.2, 39.1, 36.3, 35.5, 35.1, 33.0, 27.4, 27.2, 26.9, 25.7, 23.6, 21.0, 20.7, 17.6. IR spectrum (KBr): 3425 (NH_2); 2930, 2865 (CH_2); 1098 (COC). MS (ESI) *m/z*: 320.3 (100%, M+1). HR-MS (ESI) *m/z* for $C_{21}H_{38}NO$ [M+1] calcd. 320.29479, found 320.29456.

2.2. Biochemistry

2.2.1. Chemicals

Bacteriological agar, charcoal stripped fetal bovine serum (DCC-FBS), ethidium bromide, fetal bovine serum (FBS), glutamine, Luria Bertani (LB) broth, lymphocyte separation medium 1077, lysostaphin, Mueller Hinton (MH) broth, resazurin, and Roswell Park Memorial Institute (RPMI) medium (Thermo Fisher Scientific) were purchased from Merck. Ciprofloxacin, erythromycin, and dimethylsulphoxide (DMSO) were purchased from Penta (Czech Republic). In addition, the following chemicals were used: boeravinon B (MedChemExpress, Monmouth Junction, NJ, USA), minimum essential medium (MEM; Thermo Fisher Scientific), ONE-Glo EX Luciferase Assay System solution (Promega, Madison, WI, USA), and RNAlater (Invitrogen, Waltham, MA, USA).

2.2.2. Bacterial strains and tissue cultures

Clinical *S. aureus* isolates were obtained from the collections of microorganisms at the Department of Medical Microbiology, Motol University Hospital, and at the General University Hospital, both in Prague, Czech Republic. Antibiotic susceptibility was determined according to EUCAST (v14) using the microdilution or disk diffusion method. The

following antibiotics were tested: oxacillin (OXA; penicillin), cefoxitin (FOX; cephalosporin), ciprofloxacin (CIP; fluoroquinolone), amikacin (AMK; aminoglycoside), erythromycin (ERY; macrolide), tigecycline (TGC; tetracycline), tetracycline (TET; tetracycline), linezolid (LZD; oxazolidinone), rifampicin (RIF; rifamycin), and trimethoprim (TMP; diaminopyrimidine). Bacterial identification was regularly verified using MALDI-TOF mass spectrometry (Autoflex Speed, Bruker).

All strains used were classified as multidrug resistant (MDR) and also methicillin-resistant *S. aureus* (MRSA). Strain M960 (resistant to OXA, FOX, CIP, ERY) belonged to the clonal complex ST8, *spa* type t008, SCC*mec* type IVa, and its genome sequence was submitted to the BioSample database (NCBI, https://www.ncbi.nlm.nih.gov/biosample) under accession number SAMN51331743. Strain M53 was characterized as resistant to OXA, FOX, CIP; clonal complex ST8, *spa* type t008, SCC*mec* type Iva; accession number SAMN51331742. Strain SA4 was resistant to OXA, FOX, TMP, TGC, TET; clonal complex ST22, *spa* type t223, SCC*mec* type Iva; accession number SAMN51152089, and strain M334 was resistant to OXA, FOX, ERY, TGC; clonal complex ST152, *spa* type t4019, SCC*mec* type V; accession number SAMN51155644.

Human cervical adenocarcinoma cells stably transfected with two constructs (HeLa9903), the hER alpha expression construct and a firefly luciferase reporter construct containing an Estrogen-Responsive Element (ERE), were purchased from the European Collection of Authenticated Cell Cultures (ECACC; 11033105). Human breast cancer cell line MDA-kb2 was purchased from the American Type Culture Collection (ATCC; CRL-2713).

2.2.3. General methods

2.2.3.1. Ethidium bromide accumulation assay. The accumulation of ethidium bromide (EtBr) was assessed using a fluorescence-based assay, adapted from Křížkovská et al. [36] with minor modifications. Briefly, *S. aureus* M960 was cultured overnight in the presence of ciprofloxacin or erythromycin (1 mg/L) to induce efflux pump activity. The overnight culture was diluted in phosphate-buffered saline (PBS) to $OD_{600} = 0.6$, centrifuged (13,000×*g*, 3 min), and resuspended in fresh PBS. The bacterial suspension was subsequently distributed (50 μL/well) into a black 96-well plate (Thermo Fisher Scientific). An equal volume of EtBr solution (final concentration: 1 μg/mL) with the test sample, solvent (DMSO; 1% *v/v*), or boeravinone B (21 μM) was added to each well. The fluorescence signal (530/600 nm, exc./em.) was measured kinetically for 60 min at 60 s intervals (SpectraMax iD5 Multi-Mode Microplate Reader, Molecular Devices, CA, USA). The data were evaluated as the sum of fluorescence under the curve (FUC), normalized to boeravinone B (positive control (PC); set to 1) and an equivalent volume of DMSO (negative control (NC); set to 0). The relative activity (RA) of the steroids was calculated as $100 \times (FUC_{steroid} - FUC_{NC})/(FUC_{PC} - FUC_{NC})$.

2.2.3.2. Antimicrobial activity assay. Antimicrobial activity of steroids was measured by the standardized broth microdilution method according to ISO 20776-1. The overnight culture of *S. aureus* was diluted in MH broth to a concentration of 5×10^5 colony forming units (CFU)/mL. The culture was dispensed into a 96-well plate (100 μL/well). For each steroid, 198 μL of inoculated medium were placed in the first row, and 2 μL of a 100-fold concentrated stock solution was added to reach the desired starting concentration (50 μM). A two-fold serial dilution was then prepared by transferring 100 μL from each well to the next, each containing 100 μL of the inoculated medium, resulting in a final concentration range of 50 to 1.56 μM. After 20 h of incubation (37 °C, 120 rpm), the absorbance was measured at 590 nm (Infinite 200 PRO multimode plate reader, Tecan, Switzerland). The antimicrobial activity was evaluated as the minimum inhibitory concentration (MIC; concentration inhibiting 80 % or more of the cells) using an online calculator (AAT Bioquest, Inc., CA, USA; https://www.aatbio.com/tools/ic50-calculator).

2.2.3.3. Multidrug-resistant bacterial strains sensitization assay. Sensitization was measured using a previously published procedure using the broth microdilution method, as described by Holasová et al. [37]. The overnight culture of previously characterized strain *S. aureus* SA4 was diluted in MH broth to a concentration of 5×10^5 CFU/mL. Then, ciprofloxacin (0.15 mg/L) or erythromycin (0.14 mg/L) was added to the culture at a concentration inhibiting 50 % of the cells (IC_{50}). Steroid samples were tested by two-fold serial dilution in a concentration range of 1.56 to 50 μM. After 20 h of incubation (37 °C, 120 rpm), the absorbance was measured at 590 nm (Infinite 200 PRO). The sensitization activity was evaluated as the MIC using an online calculator (AAT Bioquest, Inc.).

2.2.3.4. Checkerboard assay. The steroid-antibiotic interactions were examined using the two-dimensional broth microdilution assay to test the effect of these compounds against previously characterized strains *S. aureus* SA4, M53, and M334. The overnight culture of the bacterial strain was diluted in MH broth to a concentration of 5×10^5 CFU/mL and dispensed into a 96-well plate. 0.75-fold serial dilutions of the antibiotic (ciprofloxacin or erythromycin) were performed horizontally across columns 2 to 6, while 0.75-fold serial dilutions of the steroid were performed vertically across rows B to F, generating a concentration matrix of both agents. The tested concentration ranges of both compounds were selected based on their previously determined individual MIC values, ensuring that the highest tested concentration exceeded the MIC, while at least the third dilution step fell below it. Column 7 contained wells only with the steroid, and row G contained wells only with the antibiotic. Columns 9 to 11 served as negative growth controls, consisting of bacterial inoculum in MH broth without any added compounds. After 20 h of incubation (37 °C, 120 rpm), the absorbance was measured at 590 nm. The fractional inhibitory concentration index (FICI) was calculated for each combination according to the formula [38]:

$$FICI = \left(\frac{MIC_A \text{ in combination}}{MIC_A \text{ alone}}\right) + \left(\frac{MIC_B \text{ in combination}}{MIC_B \text{ alone}}\right)$$

where MIC_A and MIC_B refer to the minimum inhibitory concentrations of the steroid and the antibiotic, respectively. The interaction was interpreted as synergistic (FICI $\leq$0.5), additive (0.5 < FICI $\leq$1), indifferent (1 < FICI $\leq$4), or antagonistic (FICI >4).

2.2.3.5. Cytotoxicity assay. Peripheral blood mononuclear cells (PBMCs) were isolated from the blood of healthy donors. PBMCs were taken and maintained in accordance with the ethical principles of UCT Prague, established by the Code of Ethics of UCT Prague (Ethics committee approval ID: EC 6/25) and with the principles of the Helsinki Declaration of 1964 (Ethical principles Research Involving Human Subjects). Blood was collected into tubes containing EDTA to prevent coagulation and processed within 2 h. PBMCs were isolated using a density gradient centrifugation method. Specifically, 15 mL of lymphocyte separation medium was added to a SepMate tube (Stemcell Technologies, Canada), followed by the slow layering of whole blood on top. The tube was centrifuged at 1200×*g* for 15 min at 20 °C.

The plasma layer, including the PBMC layer and part of the separation medium, was carefully transferred to a new 50 mL Falcon tube and diluted with PBS up to 50 mL. The suspension was centrifuged (500×*g*, 5 min, 20 °C), and the resulting cell pellet was resuspended in RPMI medium and adjusted to a final concentration of 7.5×10^5 cells/mL.

Cells were seeded into 96-well plates, and test samples were added in serial dilutions. After 72 h of incubation, cytotoxicity was assessed using a resazurin assay. Resazurin solution (0.03 mg/mL in PBS) was added to each well, and plates were incubated for 1 h. Fluorescence was measured at 560/590 nm (exc./em.). Cytotoxicity was determined by comparing fluorescence signals to untreated control wells and expressed as the concentration that inhibited cell viability by 80 % (IC_{80}).

2.2.3.6. Estrogenic, androgenic, and progestogenic activity assay. HeLa9903 and MDA-kb2 cell lines were incubated at standard conditions (37 °C, 5% CO_2, humidified atmosphere) in MEM with 10% DCC-FBS and RPMI medium with 10% FBS, respectively; both without phenol red and supplemented with 2 mM stable glutamine. HeLa9903 cells were regularly treated with a combination of G418 (800 μg/mL) and blasticidin S (16 μg/mL), and MDA-kb2 cells were regularly treated with G418 (500 μg/mL) to maintain the responsiveness.

First, the cytotoxicity of the tested substances after 24 h exposure was tested using both HeLa9903 and MDA-kb2 and evaluated using the resazurin assay. The transactivation assay was performed for androgenic receptors, both for agonistic and antagonistic effects. Assays with HeLa9903 cells expressing the estrogen receptor alpha (ERα) were performed according to the EPA [39] and OECD [40] standards. Assays with MDA-kb2 cells expressing the AR receptor were performed according to Wilson et al. [41] and the OECD standard [42].

For each assay, HeLa9903 or MDA-kb2 cells were seeded (1×10^5 or 2.5×10^4 cells per well, respectively), and 3 h after seeding, the solutions of tested substances (final concentration: 10 μM) and/or the control substances (Supplementary Table S1) were added to the cells. Sole medium served as a negative control (NC), and DMSO (0.1–1%) in medium served as a vehicle control (VC). After 24h incubation, ONE-Glo EX Luciferase Assay System solution was added to the wells, and luminescence was measured using Synergy H1 (BioTek Instruments, VT, USA). Results were expressed as fold induction (FI), *i.e.* fold increase compared to vehicle control. According to EPA [39], the FI of the positive control should be above 4 to meet the performance standard.

For the agonistic assay, the concentration range of a proven agonist was added to confirm the responsiveness of the cells. Increased activity in the presence of the tested substance was considered an agonistic effect. For the antagonistic assay, cells were stimulated with a fixed concentration of agonist, and the concentration range of the proven antagonist was added. Decreased activity in the presence of the agonist plus the tested substance was considered an antagonistic effect.

Both agonistic and antagonistic effects of steroid derivatives on ERα and estrogen receptor beta (ERβ) and progesterone receptors (PR) were evaluated using a contract-based service (Eurofins Scientific, Luxembourg). The assays were performed using human recombinant receptors expressed in insect cells and analyzed by Time-Resolved Förster Resonance Energy Transfer (TR-FRET) coactivator assay, according to the provider's validated protocols: 311410 ERα, 311440 ERβ, 338270 PR.

2.2.3.7. Transcriptomic assay. Biological triplicates ($n = 6$ per condition, including control) of *S. aureus* SA4 were grown by diluting overnight cultures 1:100 into 3 mL of fresh MH broth and cultivated to a 3.0 McFarland standard. Cultures were then treated with test compounds (antibiotic, steroid, or both) and incubated for an additional 2 h. Concentrations were chosen according to the checkerboard assay for each given combination and are explicitly listed in Table 1. Cells were pelleted and preserved in RNAlater. Total RNA was extracted using the RNeasy Plus Mini Kit (Qiagen, Germany), with lysostaphin-mediated lysis as the initial step. cDNA libraries were prepared following the protocol by Grunberger et al. [43], omitting terminator exonuclease treatment. Barcoded samples were sequenced on MinION and PromethION flow cells (Oxford Nanopore Technologies, UK) for 72 h. Basecalling and demultiplexing were performed using Dorado v7.6.7 (Oxford Nanopore Technologies). Transcript quantification was conducted with Salmon v1.10.3 [44] using a custom reference genome assembled *de novo* with Flye [45] and annotated with Bakta [46]. Differential expression analysis was performed with DESeq2 v1.46.0 (Bioconductor R package, MA, USA). Results were visualized using EnhancedVolcano (Bioconductor R package), Cytoscape with STRINGapp (Cytoscape Foundation, CA, USA), and ggplot2 (Comprehensive R Archive Network; CRAN).

Table 1
Minimal inhibitory concentrations (MICs) of *S. aureus* SA4 after exposure to steroids alone or in combination with ciprofloxacin (CIP) at its IC_{50} concentration (0.14 mg/L). Data are presented as mean ± standard error of the mean (SEM) from three independent replicates.

Compound	Sample alone	Sample in combination with CIP (IC_{50})
	MIC [μM]	MIC [μM]
13	94.84 ± 0.15	17.12 ± 1.17
16	67.20 ± 0.61	36.33 ± 1.48
17	61.45 ± 0.24	23.67 ± 0.17
19	52.43 ± 0.42	24.00 ± 0.29

For concentrations in μg/mL, see Supplementary Table S16.

2.2.3.8. Computational analysis of steroid-antiporter interactions. The efflux antiporter of *S. aureus* has no experimentally determined structure deposited in the Protein Data Bank (PDB). Its UniProt entry (A0A0U1MT24_STAAU) contains only a predicted model. Therefore independent structure predictions using several AI-based modeling tools: Boltz 2 [47], AlphaFold 3, ESMFold, and OmegaFold, was generated. To explore possible interaction sites, we performed co-folding simulations with Boltz 2 and AlphaFold 3, complemented by AI-based binding site prediction using DiffDock. Since AI-based binding predictions are approximate, the ligand poses using conventional molecular docking with AutoDock Vina was refined [48]. The predicted AI-derived pockets served as initial search regions. To further assess the stability of the predicted ligand-antiporter complexes, all-atom molecular dynamics simulations (100 ns) using OpenMM was performed [49].

3. Results and discussion

3.1. Sensitization screening using steroid–antibiotic combinations

The panel of steroids shown in Fig. 1 was tested in combination with five clinically relevant antibiotics representing different classes and mechanisms of action: oxacillin, gentamicin, tetracycline, ciprofloxacin, and erythromycin. The selected antibiotics are known to be excreted from cells by efflux pumps, most commonly from the major facilitator superfamily (MFS; *e.g.*, LmrS [50]; tetA, tet38 [51]; NorA, NorB, NorC [52]) and ATP-binding cassette (ABC) family (*e.g.*, AbcA [50]; MsrA [50]).

The measurements were performed according to the method described in Section 2.2.3.3. using *S. aureus* SA4. For oxacillin and tetracycline, the breakpoint concentrations defined by EUCAST clinical breakpoints (v14.0) were used, as the tested *S. aureus* strain exhibited resistance to these antibiotics (2 mg/L and 1 mg/L, respectively). For ciprofloxacin and erythromycin, concentrations corresponding to the IC_{50} values were applied (0.15 mg/L and 0.14 mg/L, respectively).

While no significant sensitizing effects were observed in combinations with oxacillin, gentamicin, or tetracycline, two antibiotics (ciprofloxacin and erythromycin) showed notable reductions in MIC when co-applied with pregnanolone and 5β-pregnane-3,20-dione (Supplementary Table S2). Interestingly, both of these antibiotics are known substrates of the LmrS efflux pump, which contributes to macrolide and fluoroquinolone resistance in *S. aureus* [53,54]. Whole genome sequencing analysis revealed that the *S. aureus* SA4 strain used in this study harbors 11 putative efflux pumps (Supplementary Table S3), of which only LmrS is capable of exporting both antibiotics. The observed MIC reductions in the presence of selected steroidal compounds suggest that they may interfere with this basal efflux activity. These preliminary findings prompted further evaluation using a specialized ethidium bromide (EtBr) efflux inhibition assay and a sensitization assay, both of which were systematically applied throughout the structure-activity relationship (SAR) study.

3.2. Structure-activity relationship study based on natural steroid hormones and neurosteroids

First, we evaluated a library of endogenous steroidal compounds (Fig. 1) to determine their potential to inhibit efflux activity in *S. aureus* M960. Although this strain is resistant to ciprofloxacin (due to a *gyrA* mutation) and erythromycin (*via* ErmC), its highly MDR phenotype is associated with increased efflux pump activity. For this reason, it served as as a model organism for studying EtBr accumulation resulting from efflux pump inhibition.

The activity of endogenous steroids to inhibit the staphylococcal efflux pump system was assessed primarily using the EtBr accumulation assay, which provides a sensitive fluorescence-based readout. Among all tested compounds, pregnanolone was identified as the most active compound (Fig. 2), reaching over 20% of the activity observed with the positive control boeravinone B, clearly outperforming all other tested steroids. Progesterone, the biosynthetic precursor of pregnanolone, also showed notable activity, supporting the relevance of this structural motif.

Pregnanolone is a 3α,5β-reduced analog of progesterone. In healthy women, progesterone can be reduced into various metabolites (Fig. 3A). Approximately 50 % of progesterone is reduced to 5α-dihydroprogesterone *via* the enzyme 5α-reductase, 35 % to 3β-hydroxyprogesterone, and 10 % to (20*S*)-dihydroprogesterone (also reffered to in the literature as 20α-dihydroprogesterone) [55].

The 3-oxo group of 5α-dihydroprogesterone is reduced to a 3α-hydroxyl substituent by 3α-hydroxysteroid-oxidoreductase, affording endogenous neurosteroid allopregnanolone [11,56], or, to a lesser extent, the endogenous neurosteroid isopregnanolone, which carries a 3β-hydroxy group. Similar to the 5α-steroid reductase pathway, progesterone can be metabolized *via* the 5β-pathway by the AKR1D1 enzyme (aldo-keto reductase (AKR) family) [57], yielding pregnanolone and epipregnanolone (Fig. 3A). However, this metabolic pathway is minor and predominates in the peripheral compartment of the central nervous system [58]. The most important and well-studied 5β-reduced steroids are bile acids, whose biosynthesis serves as a major route for cholesterol metabolism. Historically, it was believed that the 5β-pathway was involved in steroid inactivation [59]. It is now recognized, however, that 5β-reduced steroids are not inactive; they act as ligands for orphan nuclear receptors [60] and modulate the activities of the $GABA_A$ and NMDA receptors [61].

The absolute stereochemistry at positions C-3 and C-5 of allopregnanolone, isopregnanolone, pregnanolone, and epipregnanolone is defined by these chiral centers. The 5α-steroids have a *trans* fusion of the A/B-rings, as the C-5 proton and the C-10 angular methyl are oriented oppositely (allopregnanolone and isopregnanolone). Consequently, this skeleton is described as a "planar" steroid (Fig. 3A). The "bent" steroids are compounds with a *cis* fusion of the A/B-rings, as the C-5 proton and the C-10 angular methyl are oriented on the same side (pregnanolone and epipregnanolone). Regarding the stereochemistry at position C-3, the 3α-substituent lies below the steroidal plane (represented as a dashed bond), while the 3β-substituent lies above the plane (represented as a solid wedge).

To assess the functional relevance of these stereochemical configurations, we compared the EtBr accumulation levels observed for individual progesterone metabolites (Fig. 3B). Pregnanolone again exhibited the strongest effect, followed by its precursor 5β-pregnane-3,20-dione. In contrast, the 5α-reduced analogues allopregnanolone and isopregnanolone displayed substantially lower activity. These findings suggest that the 3α,5β-configuration, corresponding to the bent A/B-ring conformation, enhances the ability of these compounds to inhibit efflux in *S. aureus*. Based on these results, pregnanolone was selected as the scaffold for subsequent structural derivatization as part of the structure-activity relationship (SAR) study (Fig. 4).

Two main structural features of pregnanolone were evaluated in the SAR study, *i.e.* modifications at positions C-3 (Fig. 5A) and C-17 (Fig. 6A). The C-3 hydroxyl group of the steroidal skeleton was modified with negatively charged (compound **1**), positively charged (compound **2**), zwitterionic (compound **3**), and uncharged (compound **4**) substituents, respectively (Fig. 5A).

To further evaluate the efflux-inhibitory potential of pregnanolone-based derivatives, two complementary assays were performed. EtBr accumulation served as a primary indicator of efflux inhibition in ciprofloxacin-induced *S. aureus*. In parallel, the functional relevance of this inhibition was assessed by determining the MIC values of each derivative alone and in combination with ciprofloxacin at its IC_{50} (0.15 mg/L). A significant reduction in MIC under combinatorial conditions indicates sensitization of the bacterial strain and thus provides

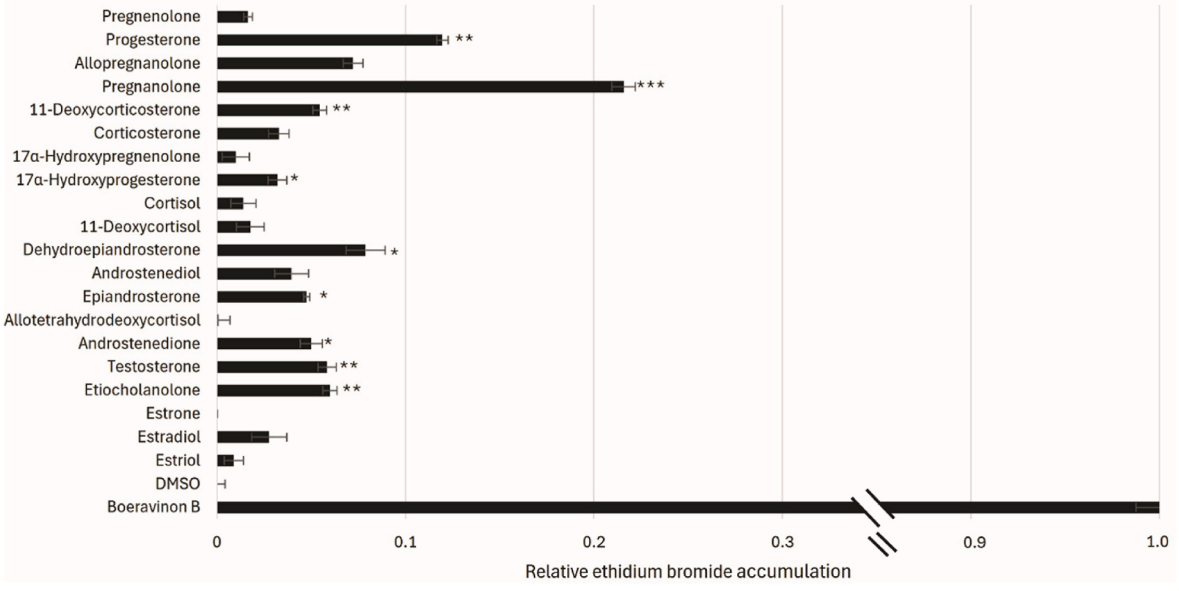

Fig. 2. Relative accumulation of ethidium bromide in ciprofloxacin-induced *S. aureus* M960 caused by endogenous steroids, boeravinon B (positive control, 21 μM), and DMSO (negative control). Steroids were tested at a concentration of 50 μM. Data are presented as the average of three replicates ± standard error of the mean (SEM). The effect of steroids was analyzed using a two-tailed *t*-test. Statistically significant differences from the negative control are indicated with * ($p \leq 0.01$), ** ($p \leq 0.001$), *** ($p \leq 0.0001$). For concentrations in μg/mL, see Supplementary Table S4.

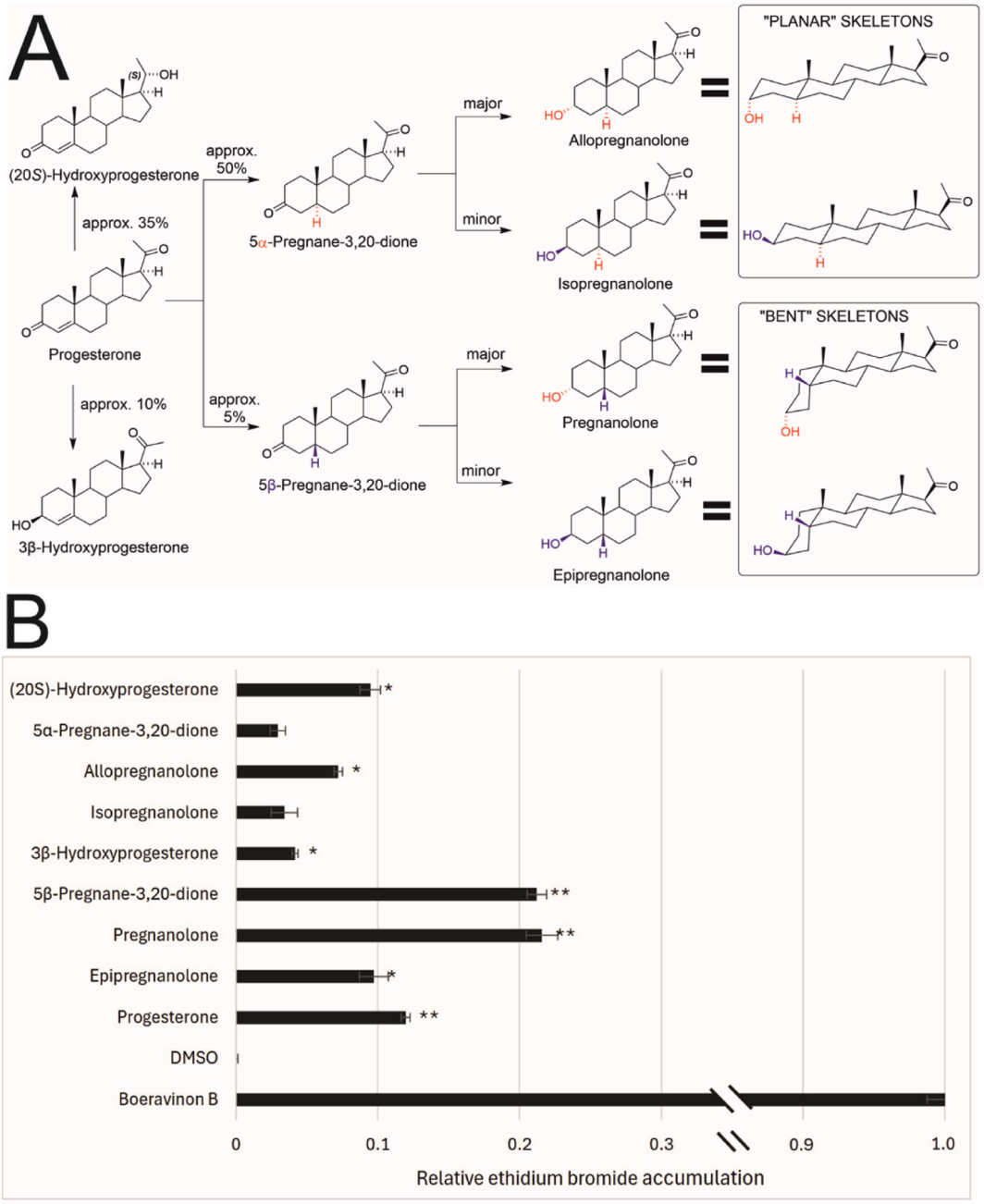

Fig. 3. *(A)* Structure of metabolites of progesterone. *(B)* Relative accumulation of ethidium bromide in ciprofloxacin-induced *S. aureus* M960 caused by endogenous steroids, boeravinon B (positive control, 21 μM), and DMSO (negative control). Steroids were tested at a concentration of 50 μM. The effect of steroids was analyzed using a two-tailed *t*-test. Statistically significant differences from the negative control are indicated with * ($p \leq 0.01$), ** ($p \leq 0.001$). For concentrations in μg/mL, see Supplementary Table S5.

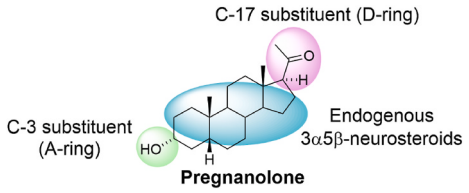

Fig. 4. Structural representation of pregnanolone with highlighted key positions targeted in the SAR study design.

confirmatory evidence of efflux pump inhibition.

Among the tested derivatives, only compound **4** exhibited a significant increase in EtBr accumulation, exceeding even the level of the positive control (Fig. 5B), indicating potent inhibition of efflux activity. Importantly, this effect translated into a reduction of the MIC when combined with ciprofloxacin at its IC_{50} concentration (Fig. 5C), suggesting that compound **4** is capable of sensitizing the multidrug-resistant *S. aureus* strain to this antibiotic.

As mentioned previously, two main structural features of pregnanolone can be evaluated, *i.e.* modifications at positions C-3 and C-17 (D-ring; Fig. 4). To probe the impact of lipophilicity, which can be modified by nonpolar substituents of the D-ring, a series of compounds **5**–**8** was synthesized and evaluated (Fig. 6A). It should be noted that once the C-17 acetyl side chain of the pregnane skeleton is removed, the resulting structure is referred to as androstane. We hypothesized that the

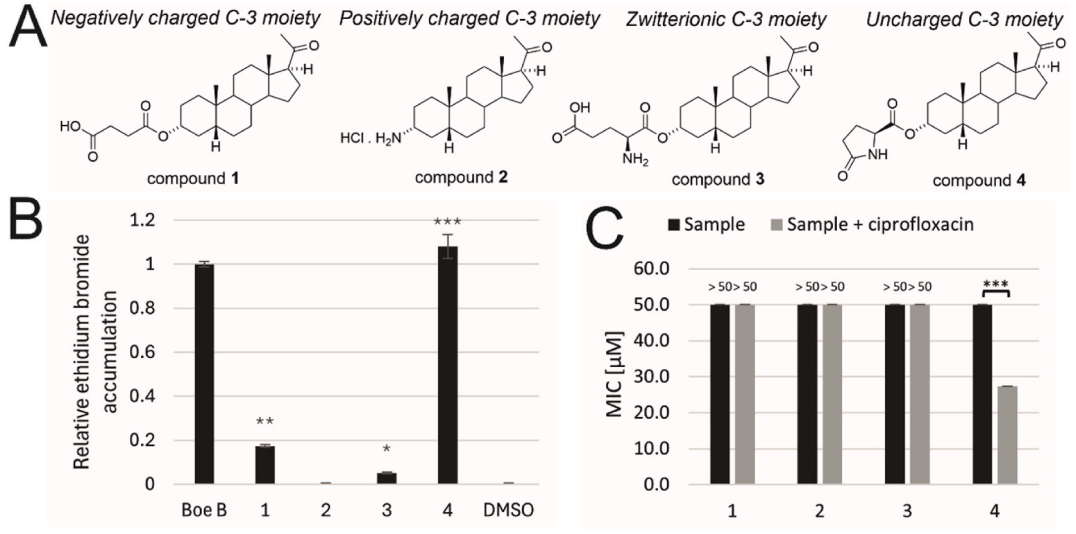

Fig. 5. *(A)* Structures of pregnanolone compounds **1**–**4** modified at position C-3 (A-ring). *(B)* Relative accumulation of ethidium bromide in ciprofloxacin-induced *S. aureus* M960 caused by steroid derivatives **1**–**4**, boeravinon B (Boe B; positive control, 21 μM), and DMSO (negative control). Steroids were tested at a concentration of 50 μM. The effect of steroids was analyzed using a two-tailed *t*-test. Statistically significant differences from the negative control are indicated with * ($p \leq 0.01$), ** ($p \leq 0.001$), *** ($p \leq 0.0001$). *(C)* Minimum inhibitory concentration (MIC, μM) of steroidal compounds tested against *S. aureus* SA4, alone and in combination with ciprofloxacin IC_{50} (0.15 mg/L). Steroids were evaluated in a concentration range of 1.56–50 μM. Data are presented as the average of three replicates ± standard error of the mean (SEM). The effect of steroids was analyzed using a two-tailed *t*-test. Statistically significant differences between derivative MIC and derivative MIC in the presence of ciprofloxacin are indicated with *** ($p \leq 0.0001$). For concentrations in μg/mL, see Supplementary Table S6–S7.

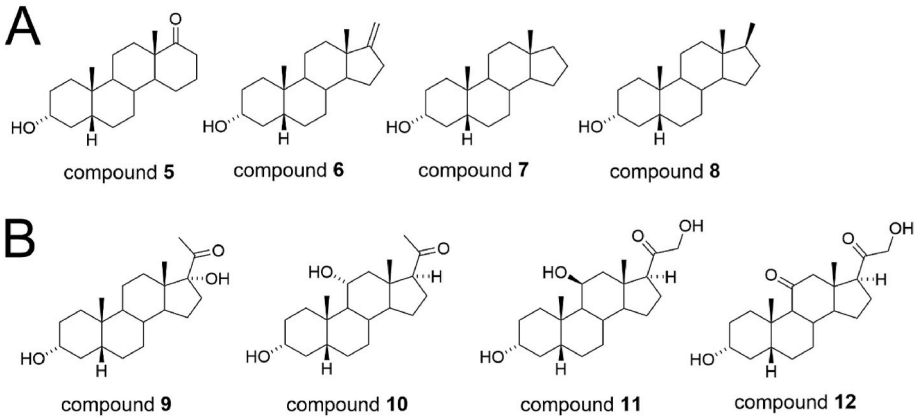

Fig. 6. *(A)* Structures of androstane derivatives **5**–**8** modified in the D-ring and *(B)* structures of endogenous 3α,5β-neurosteroids **9**–**12** with natural substituents at positions C-11 and C-17.

increased lipophilicity might correlate with altered steroid accumulation in the plasma membrane and, consequently, with the biological effect [28,30]. However, none of the analogues **5**–**8** exhibited any measurable increase in EtBr accumulation or reduction in MIC values under combinatorial conditions with ciprofloxacin (Supplementary Fig. S39). To further explore the structural requirements, additional endogenous 3α,5β-neurosteroids (compounds **9**–**12;** Fig. 6B), bearing substituents at positions C-11 and C-17, were tested. However, these compounds likewise failed to elicit any significant effect on EtBr accumulation or reduction in MIC values under combinatorial conditions with ciprofloxacin (Supplementary Fig. S39). Taken together, these results indicate that neither increased lipophilicity at the D-ring nor native steroidal substitutions at key positions are sufficient to induce efflux pump inhibition or sensitization in *S. aureus*.

To exclude the possibility that a combination of modifications at C-3 and C-17 might be required, we subsequently prepared compounds bearing substitutions at both positions (compounds **13**–**16**; Fig. 7A). This design aimed to assess potential additive or synergistic effects between modifications at these two key positions. Interestingly, derivatives **13** and **16** exhibited strong efflux pump inhibition, with EtBr accumulation reaching levels coparable to the positive control (Fig. 7B). Importantly, both compounds significantly lowered the MIC of ciprofloxacin when administered in combination, effectively reversing the ciprofloxacin-resistant phenotype of *S. aureus* (Fig. 7C). In contrast, compounds **14** and **15**, while also showing moderate efflux inhibition, exhibited intrinsic antibacterial activity, with very low MIC values even in the absence of ciprofloxacin. However, their combination with the antibiotic did not further enhance susceptibility, indicating that their effect is likely independent of efflux modulation. Taken together, these results identify two active derivatives, compounds **13** and **16**, which displayed synergistic effects arising from modifications at both positions.

3.3. Structural modifications of compounds 13 and 16

Building on these findings, subsequent experiments focused on structural modifications of compounds **13** and **16**. The synthetic modifications were designed to further explore the structural determinants

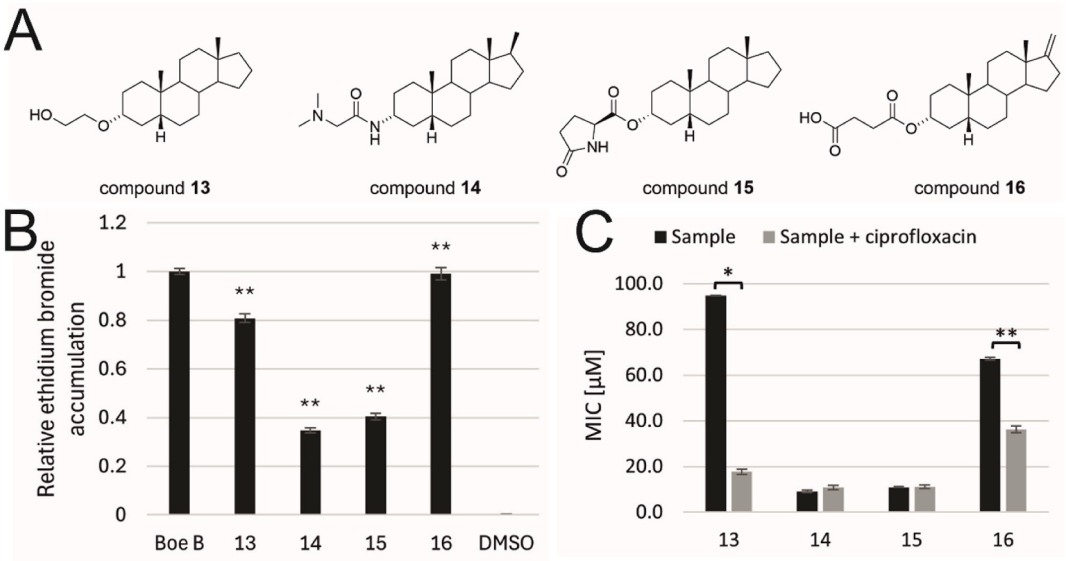

Fig. 7. *(A)* Structures of derivatives **13**–**16** with combined modifications in both positions C-3 and C-17. *(B)* Relative accumulation of ethidium bromide in ciprofloxacin-induced *S. aureus* M960 caused by steroid derivatives, boeravinon B (Boe B; positive control, 21 μM), and DMSO (negative control). Steroids were tested at a concentration of 50 μM. The effect of steroids was analyzed using a two-tailed *t*-test. Statistically significant differences from the negative control are indicated with ** ($p \leq 0.001$). *(C)* Minimum inhibitory concentration (MIC, μM) of steroidal compounds tested against *S. aureus* SA4, alone and in combination with ciprofloxacin at its IC_{50} concentration (0.15 mg/L). Steroids were evaluated in a concentration range of 1.56–50 μM. Data are presented as the average of three replicates ± standard error of the mean (SEM). The effect of steroids was analyzed using a two-tailed *t*-test. Statistically significant differences between derivative MIC and derivative MIC in presence of ciprofloxacin are indicated with * ($p \leq 0.01$), ** ($p \leq 0.001$). For concentrations in μg/mL, see Supplementary Table S8–S9.

underlying the observed synergistic effects and to assess whether additional modifications could enhance efflux inhibition or sensitizing potential.

In line with our previous SAR approach, we first examined the structural requirements of the C-3 substituent in compound **16** by comparing a three-carbon substituent (hemimalonate, **17**), a four-carbon substituent (hemisuccinate, **16**), and a five-carbon substituent (hemiglutarate, **18**). Both compounds **17** and **18** showed strong efflux-inhibitory activity, with EtBr accumulation levels comparable to those of the positive control and compound **16** (Fig. 8B). Importantly, their MIC values in the presence of ciprofloxacin decreased to approximately 25 μM, compared with 36 μM for compound **16**, indicating that C-3 modification further enhanced the antibacterial potential of the steroid (Fig. 8C).

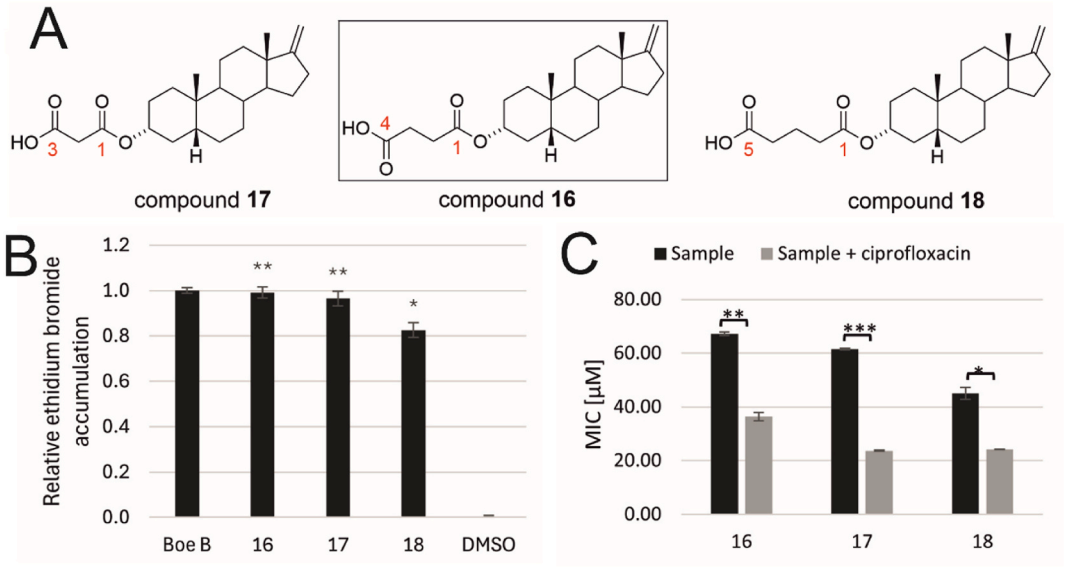

Fig. 8. *(A)* Structures of compounds **16**–**18** with various hemiester modifications at position C-3 (A-ring). *(B)* Relative accumulation of ethidium bromide in ciprofloxacin-induced *S. aureus* M960 caused by steroid derivatives, boeravinon B (Boe B; positive control, 21 μM), and DMSO (negative control). Steroids were tested at a concentration of 50 μM. The effect of steroids was analyzed using a two-tailed *t*-test. Statistically significant differences from the negative control are indicated with * ($p \leq 0.01$), ** ($p \leq 0.001$). *(C)* Minimum inhibitory concentration (MIC, μM) of steroidal compounds tested against *S. aureus* SA4, alone and in combination with ciprofloxacin at its IC_{50} concentration (0.15 mg/L). Steroids were evaluated in a concentration range of 1.56–50 μM. Data are presented as the average of three replicates ± standard error of the mean (SEM). The effect of steroids was analyzed using a two-tailed *t*-test. Statistically significant differences between derivative MIC and derivative MIC in the presence of ciprofloxacin are indicated with * ($p \leq 0.01$), ** ($p \leq 0.001$), *** ($p \leq 0.0001$). For concentrations in μg/mL, see Supplementary Table S10–S11.

As compounds **16**–**18** exhibited comparable MIC values, the C-3 hemisuccinate moiety was selected for further modifications owing to its convenient synthesis. Accordingly, new derivatives were synthesized bearing a C-3 hemisuccinate moiety in combination with various C-17 subsitituions (compounds **19** and **20**; Fig. 9A) and core skeleton modifications while retaining the pregnane C-17 acetyl substituent (compounds **21**–**23**; Fig. 9A). Among these, only compound **19** displayed strong efflux-inhibitory effects, with EtBr accumulation levels comparable to those of the positive control and compound **16**. In contrast, compounds **20**–**23** showed only weak or moderate efflux inhibition and did not alter MIC values under combinatorial conditions. Notably, the MIC value of compound **19** was markedly reduced in the presence of ciprofloxacin, indicating a clear sensitizing effect. These results suggest synergy between the D-ring nonpolar modification and the C-3 hemiester moiety. Therefore, a series of analogues with nonpolar modifications at C-17 bearing a three-carbon substituent (hemimalonate, **24**), a four-carbon substituent (hemisuccinate, **25**), and a five-carbon substituent (hemiglutarate, **26**) was tested (Fig. 9B). Compounds **24**–**26** exhibited strong efflux-inhibitory effects, with EtBr accumulation levels comparable to those of the positive control and compound **16,** as reflected in their low MIC values when tested alone. Notably, compound **25** further enhanced ciprofloxacin efficacy, resulting in a statistically significant MIC reduction.

In summary, these findings demonstrate that the 3α,5β-steroidal skeleton permits multiple synthetic modifications that produce strong efflux-inhibitory effects in the EtBr accumulation assay, with activity levels comparable to those of the positive control. The sensitizing effect was further supported by the reduction in MIC values in the presence of ciprofloxacin. Efflux inhibition is preserved across various C-3 hemiester derivatives and can be significantly enhanced through appropriate D-ring modifications with nonpolar substituents. Importantly, C-3 and C-17 modifications are not additive, and a comprehensive series covering all possible combinations would be required to fully evaluate their interactions; an undertaking that poses a considerable synthetic challenge.

In the final part of our SAR study, we focused on structural modifications of compound **13**. Our previous results demonstrated a synergistic effect of nonpolar substitutions at C-17; therefore, for compound **13**, we investigated only modifications at the C-3 hydroxyl group. As shown in Fig. 5, the uncharged C-3 moiety of L-pyroglutamic acid afforded the most pronounced inhibitory effect. Based on this observation, we prepared a series of analogues (compounds **27**–**30**) incorporating L-pyroglutamic acid and its six-membered 6-oxopiperidine analogue (Fig. 10A). These uncharged substituents were introduced either *via* an ester bond (compounds **27** and **28**) or an amide bond (compounds **29** and **30**).

All derivatives **27**–**30** showed moderate efflux-inhibitory activity, with EtBr accumulation levels slightly below but approaching those of the positive control (Fig. 10B). Compounds **27** and **28** exhibited strong antibacterial activity, and for compound **27**, co-treatment with ciprofloxacin further reduced MIC, indicating a sensitizing effect. In contrast, compounds **29** and **30** remained inactive under the tested conditions, with MIC values exceeding 50 μM both alone and in combination (Fig. 10C).

From the SAR analysis, most of the tested derivatives exhibited negligible efflux inhibition or no measurable impact on antibiotic susceptibility and were therefore not considered for further studies. In contrast, derivatives **13**, **16**, **17**, and **19** demonstrated the most prominent efflux-inhibitory and sensitization profiles, evidenced by a significant increase in EtBr accumulation together with a consistent reduction in antibiotic MICs (Table 1). Derivatives **13** and **16** were defined as lead structures, while compound **17** underscored the importance of polar substitution at C-3, and compound **19** was included as a representative of C-17 modifications. Other compounds, such as **14**, **15**, and **24**–**26**, showed very low MIC values mainly due to direct antimicrobial activity, whereas compounds **27**–**30** exhibited only marginal effects.

3.4. Checkerboard assay

Based on the results of the SAR study, four representative compounds (**13**, **16**, **17**, **19**) showing the most promising efflux-inhibitory and sensitizing profiles were selected for further evaluation using a checkerboard assay (Table 2). The aim was to investigate potential synergistic or additive interactions with ciprofloxacin across three different MDR *S. aureus* strains.

The checkerboard assay revealed strain-dependent interaction patterns between selected steroidal compounds and ciprofloxacin. Although all three *S. aureus* MDR strains tested (SA4, M334, and M53) are multidrug-resistant, only SA4 and M334 are susceptible to ciprofloxacin. In contrast, M53 harbours resistance-conferring mutations in the *gyrA* gene, rendering it ciprofloxacin-resistant.

Compounds **13, 16,** and **17** exhibited FICI values equal to or less than 1 in both SA4 and M334, indicating additive effects. Compound **13** displayed the most consistent additive effect across the two susceptible strains. In contrast, compound **19** showed indifferent interactions in all three strains (FICI >1), suggesting limited combinatorial potential. In the ciprofloxacin-resistant M53 strain, all tested combinations led to indifferent interactions, emphasizing that the observed additive effects depend on efflux pump activity only when no mutation is present in the target site of ciprofloxacin action, *i.e.* in *gyrA*.

Taken together, these results indicate that certain steroidal compounds, particularly compound **13**, can enhance the efficacy of ciprofloxacin in multidrug-resistant *S. aureus* strains that retain susceptibility to the antibiotic. Such combinations may offer a useful strategy for preserving fluoroquinolone efficacy and delaying the emergence or spread of resistance.

3.5. Modulation of erythromycin resistance and efflux in S. aureus

In erythromycin-induced MDR M960, EtBr accumulation assays (Supplementary Fig. S40A–S44A) showed the same SAR pattern as with ciprofloxacin. Among the endogenous steroids, pregnanolone was again the most active inhibitor, while several others, previously inactive under ciprofloxacin induction, also showed notable effects (Supplementary Fig. S40).

Among the synthetic derivatives, compounds **13** and **16** displayed the highest efflux inhibition (Supplementary Fig. S42A), comparable to boeravinone B, and significantly reduced the MIC of erythromycin (Supplementary Fig. S42B). Compound **17** was also active in both assays (Supplementary Fig. S43). Compounds **14, 15, 24**–**26**, and **27**–**30** increased EtBr accumulation but lacked corresponding sensitization; for these steroids, MIC reduction was mainly due to intrinsic antibacterial activity (Supplementary Fig. S42–S44). Checkerboard assays in erythromycin-susceptible strains confirmed an additive effect for compound **13**, consistent with inhibition of the same efflux system observed for ciprofloxacin (Supplementary Table S18).

Overall, the erythromycin SAR closely mirrored that of ciprofloxacin, with pregnanolone as the lead endogenous inhibitor and compounds **13** and **16** emerging as the most potent synthetic derivatives, combining strong efflux inhibition with significant MIC reduction.

3.6. Transcriptomic analysis

Transcriptome analysis was chosen to elucidate the molecular mechanism of action of the most promising derivative, compound **13**, on bacterial cells. Transcriptome sequencing of MDR SA4 cultures, including untreated controls and those exposed to ciprofloxacin, erythromycin, compound **13**, or their combinations, revealed distinct transcriptional changes. The most significant shift was observed following erythromycin treatment, which was characterized by widespread upregulation of ribosomal protein genes (Fig. 11, Supplementary Fig. S5), consistent with the fact that erythromycin inhibits ribosomal protein synthesis. The first defence mechanism of the cell against

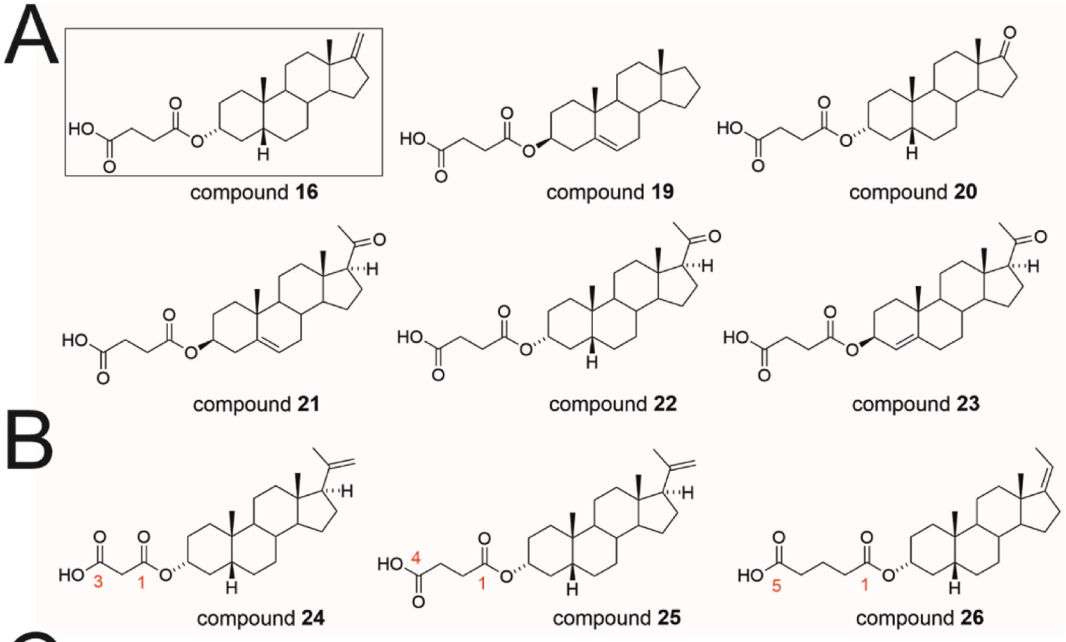

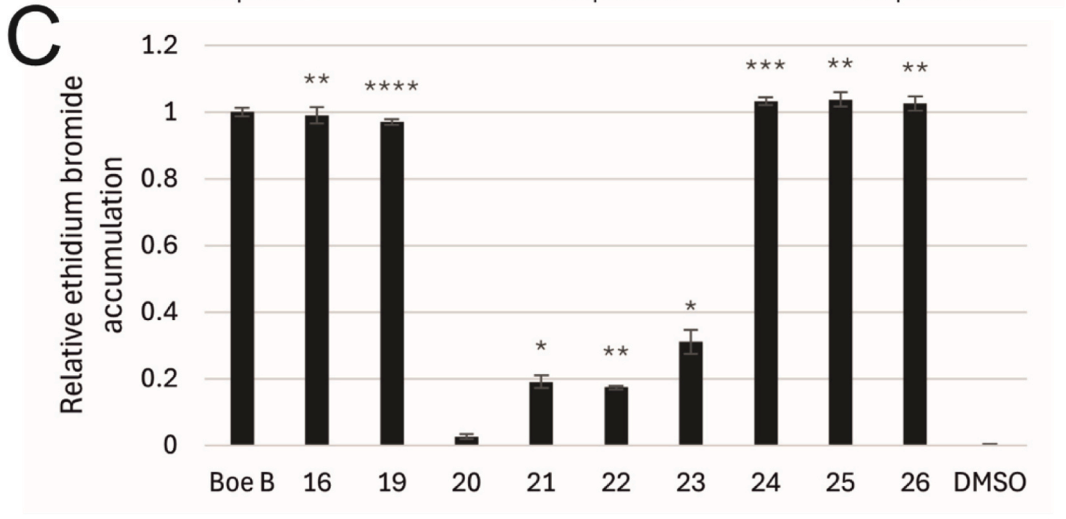

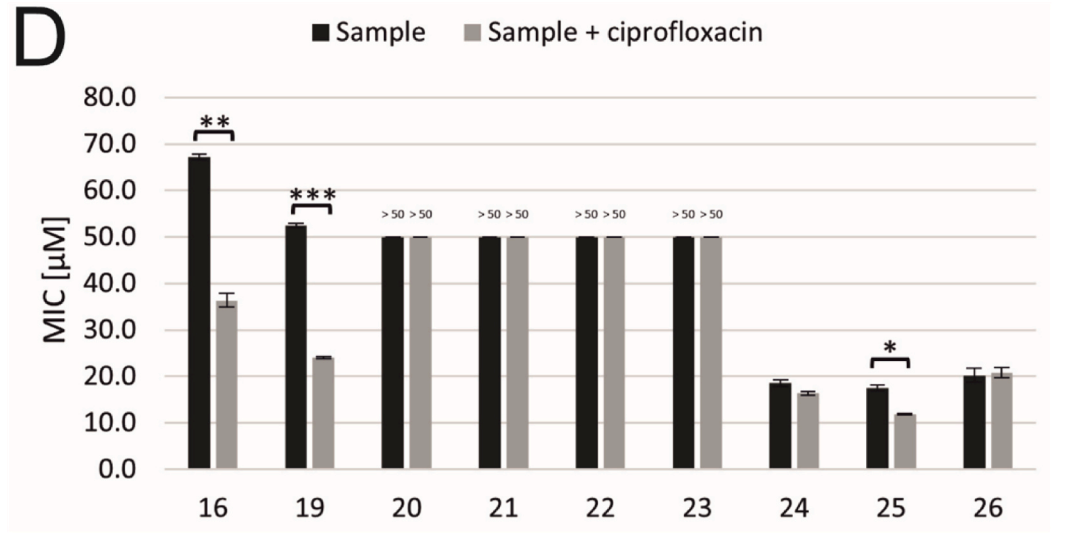

(caption on next page)

Fig. 9. *(A)* Structures of analogues **19**–**26** of compound **16** modified at positions C-17 (D-ring) and both positions C-3 (A-ring). *(B)* Structures of analogues modified at positions C-17 (D-ring) and C-3 with various hemiesters moieties. *(C)* Relative accumulation of ethidium bromide in ciprofloxacin-induced *S. aureus* M960 caused by steroid derivatives, boeravinon B (Boe B; positive control, 21 μM) and DMSO (negative control). Steroids were tested at a concentration of 50 μM. The effect of steroids was analyzed using a two-tailed *t*-test. Statistically significant differences from the negative control are indicated with * ($p \leq 0.01$), ** ($p \leq 0.001$), *** ($p \leq 0.0001$), **** ($p \leq 0.00001$). *(D)* Minimum inhibitory concentration (MIC, μM) of steroidal compounds tested against *S. aureus* SA4, alone and in combination with ciprofloxacin at its IC_{50} concentration (0.15 mg/L). Steroids were evaluated in a concentration range of 1.56–50 μM. Data are presented as the average of three replicates ± standard error of the mean (SEM). The effect of steroids was analyzed using a two-tailed *t*-test. Statistically significant differences between derivative MIC and derivative MIC in the presence of ciprofloxacin are indicated with * ($p \leq 0.01$), ** ($p \leq 0.001$), *** ($p \leq 0.0001$). For concentrations in μg/mL, see Supplementary Table S12–S13.

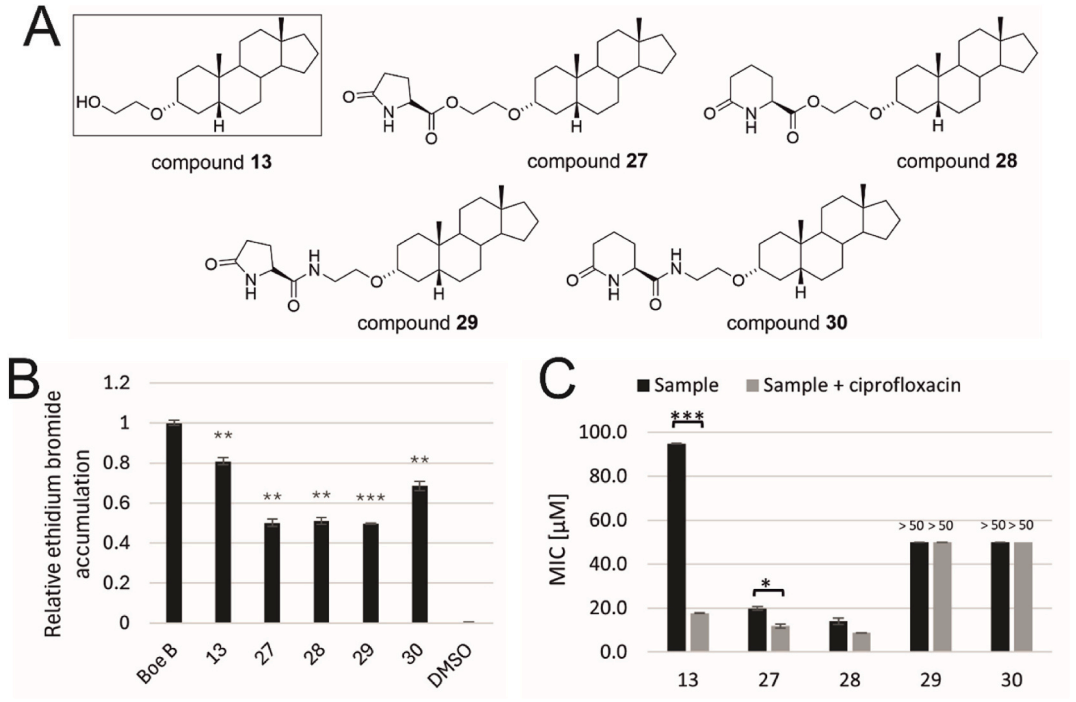

Fig. 10. *(A)* Structural analogues **27**–**30** of compound **13**. *(B)* Relative accumulation of ethidium bromide in ciprofloxacin-induced *S. aureus* M960 caused by steroid derivatives, boeravinon B (Boe B; positive control), and DMSO (negative control). Steroids were tested at a concentration of 50 μM. The effect of steroids was analyzed using a two-tailed *t*-test. Statistically significant differences from the negative control are indicated with * ($p \leq 0.01$), ** ($p \leq 0.001$), *** ($p \leq 0.0001$). *(C)* Minimum inhibitory concentration (MIC, μM) of steroidal compounds tested against *S. aureus* SA4, alone and in combination with ciprofloxacin at its IC_{50} concentration. Data are presented as the average of three replicates ± standard error of the mean (SEM). The effect of steroids was analyzed using a two-tailed *t*-test. Statistically significant differences between derivative MIC and derivative MIC in the presence of ciprofloxacin are indicated with * ($p \leq 0.01$), *** ($p \leq 0.0001$). For concentrations in μg/mL, see Supplementary Table S14–S15.

erythromycin is therefore the overproduction of its cellular target. Ciprofloxacin alone elicited a limited response, with only two genes, *sbcC* and *uvrA*, both involved in DNA repair, showing a significant increase in expression (Supplementary Fig. S45, Supplementary Table S19).

Interestingly, compound **13** itself caused a reduction in the expression of genes associated with virulence, particularly *hly* (alpha-hemolysin, often referred to in the literature as *hla*) and *psmA1-3* (phenol-soluble modulins alpha 1-3; Fig. 12) [62], while *vraX* (a secreted protein involved in complement inhibition [63]) was upregulated. It has also been reported that vraX is a very sensitive reporter of cell wall stress, and its induction is caused by cell wall-active agents [64]. This observation supports they hypothesis that compound **13** acts at the level of the cell wall or cytoplasmatic membrane, where it causes stress by inhibiting transmembrane efflux pumps. The possibility that derivative **13** acts solely through membrane destabilization was excluded using a checkerboard assay, in which its combination with vancomycin, an agent that is not a substrate of efflux pumps, did not show any interaction. Furthermore, when combined with antibiotics, compound **13** did not induce the synergistically enhanced transcriptomic response observed with the antibiotics alone, while the reduced expression of virulence-associated genes was maintained.

When cells were treated with a combination of erythromycin and derivative **13**, significant downregulation of several ribosomal genes was observed (Fig. 13B), potentially indicating interference with erythromycin-induced stress signaling, while the downregulation of virulence genes caused by compound **13** was maintained. This finding suggests a possible reduction in the virulence of bacterial strains treated with this adjuvant therapy. The ability of the proposed adjuvant therapy to inhibit virulence was verified by a reduction in staphylococcal cell adhesion (Supplementary Fig. S46) in the presence of either compound **13** alone or the adjuvant combination of compound **13** and ciprofloxacin**.** Modulation of virulence- and cell wall stress-related genes suggests that the compound may alter bacterial physiology in a manner that warrents further functional verification.

Similarly, treatment of bacterial cells with a combination of ciprofloxacin and compound **13** maintained the downregulation of virulence-associated genes but increased the expression of heat-shock proteins and certain ribosomal proteins, indicating that the cells were under stress (Fig. 13D).

3.7. Antimicrobial activity

Although the primary focus of this study was efflux inhibition and

Table 2
Fractional inhibitory concentration index (FICI) values for combinations of steroidal compounds with ciprofloxacin tested on three MDR strains (SA4, M53, M334) using the checkerboard assay. Boeravinon B (Boe B) was used as a positive control. Values represent interaction classification based on FICI: synergistic (≤0.5), additive (>0.5 to ≤ 1.0), indifferent (>1.0 to ≤ 4.0), and antagonistic (>4.0). CIP – ciprofloxacin.

steroid-ciprofloxacin interaction						
Strain	Agent	MIC		FIC	FICI	Interpretation
		Alone	Combination			
SA4	**13** [μM]	**95.00**	**18.75**	**0.20**	**0.70**	**Additive**
	CIP [mg/L]	**0.23**	**0.11**	**0.50**		
	16 [μM]	**67.10**	**37.50**	**0.56**	**0.89**	**Additive**
	CIP [mg/L]	**0.23**	**0.075**	**0.33**		
	17 [μM]	**61.30**	**37.50**	**0.61**	**0.94**	**Additive**
	CIP [mg/L]	**0.23**	**0.075**	**0.33**		
	19 [μM]	28.00	25.00	0.89	1.39	Indifferent
	CIP [mg/L]	0.23	0.11	0.50		
	Boe B [μM]	**125.00**	**3.91**	**0.03**	**0.60**	**Additive**
	CIP [mg/L]	**0.23**	**0.13**	**0.57**		
M334	**13** [μM]	**92.40**	**0.25**	**0.20**	**0.87**	**Additive**
	CIP [mg/L]	**0.15**	**0.10**	**0.67**		
	16 [μM]	**68.30**	**25.00**	**0.37**	**0.87**	**Additive**
	CIP [mg/L]	**0.15**	**0.075**	**0.50**		
	17 [μM]	**75.00**	**18.75**	**0.25**	**0.92**	**Additive**
	CIP [mg/L]	**0.15**	**0.10**	**0.67**		
	19 [μM]	37.50	25.00	0.67	1.34	Indifferent
	CIP [mg/L]	0.15	0.1	0.67		
	Boe B [μM]	**125.00**	**1.56**	**0.01**	**0.88**	**Additive**
	CIP [mg/L]	**0.15**	**0.13**	**0.87**		
M53[a]	13 [μM]	40.20	25.00	0.63	1.13	Indifferent
	CIP [mg/L]	37.50	18.75	0.50		
	16 [μM]	58.10	X	x	x	x
	CIP [mg/L]	37.50	X	x		
	17 [μM]	64.80	X	x	x	x
	CIP [mg/L]	37.50	X	x		
	19 [μM]	52.00	37.50	0.72	1.22	Indifferent
	CIP [mg/L]	37.50	18.75	0.50		
	Boe B [μM]	125.00	50	0.40	1.07	Indifferent
	CIP [mg/L]	37.50	25	0.67		

[a] Strain resistant to ciprofloxacin, x means that no combinatory effect was observed. For concentrations in μg/mL, see Supplementary Table S17.

antibiotic sensitization, several steroidal compounds were found to exert direct antimicrobial activity. Among all tested steroids, five compounds (**14**, **15**, **24**, **25**, and **26**) exhibited notably low MIC values against multidrug-resistant *S. aureus* strains.

As shown in Table 3, these compounds inhibited bacterial growth with MIC values below or around 25 μM across all three tested strains. The most potent effect was observed for compound **14**, while compound **15** also showed strong activity against both SA4 and M53.

These findings highlight that certain steroidal structures possess intrinsic antibacterial properties, independent of efflux modulation or synergistic interactions. Such compounds may represent promising leads for the development of novel antimicrobial agents targeting resistant *S. aureus* strains.

3.8. Cytotoxicity of steroids

The cytotoxic potential of the antimicrobial and adjuvant steroidal compounds was evaluated using the resazurin assay in human peripheral blood mononuclear cells (PBMCs). The resulting cytotoxicity values of the derivatives against PBMCs (MIC_{PBMCs}) were used to calculate the therapeutic index (TI), expressed as the ratio of the MIC_{PBMCs} to the MIC against *S. aureus*. For adjuvant agents, TI was expressed as the ratio of MIC_{PBMCs} to the MIC of the derivative showing the best combination effect in the checkerboard assay. For compounds that did not reach MIC at the highest tested concentration (50 μM), MIC was reported as > 50 μM, and TI was expressed as a lower-limit estimate (*e.g.*, TI > 0.74).

As shown in Supplementary Table S6, several compounds exhibited moderate cytotoxicity, with MIC_{PBMCs} ranging between 30 and 35 μM; in contrast, many compounds were non-toxic. Among the antimicrobial derivatives (Table 2), compounds **14** and **15** achieved therapeutic indeces of 3.7 and 3.0, respectively, reflecting their moderate toxicity. In contrast, compounds **24**, **25**, and **26** showed no cytotoxicity within the tested range, and their therapeutic indices were therefore higher than 2.5.

Similarly, the adjuvant compounds **16** and **17** (Table 1) did not reach MIC at the highest tested concentration (50 μM), suggesting negligible cytotoxicity under the tested conditions; their TIs are therefore higher than 2.7 and higher than 1.3, respectively. The therapeutic indices of derivatives **13** and **28** were 1.9 and 3.2, respectively.

Although the measured TI values appear relatively low, it is important to note that antimicrobial activity was determined according to the ISO standard at a bacterial dose of 5×10^5 CFU/mL, whereas bacteremia typically involves 10 to 10^4 CFU/mL in the blood [65], at least one order of magnitude lower. It can therefore be assumed that the effective adjuvant dose required *in vivo* would also be lower.

3.9. Endocrine disruption activity

As mentioned previously, steroidal hormones can modulate nuclear receptors. In contrast, neurosteroids, by definition, do not act *via* nuclear receptors. This fundamental difference in their mechanisms of action should reduce the likelihood of side effects commonly associated with steroidal hormones, such as corticosteroids. To examine the potential endocrine-disrupting activity of the tested derivatives **13**, **15**, and **16**, their ability to bind to estrogen, progesterone, and androgen receptors in human cells and act as agonists or antagonists was investigated (Supplementary Table S7).

The agonistic activity of the derivatives was compared with that of estradiol and dihydrotestosterone, both of which significantly increased fold induction (FI) even at 0.5 nM. Since there was no significant increase in FI in HeLa9903 and MDA-kb2 cells at the tested concentration (10 μM), it can be concluded that the derivatives do not interact with estrogen or androgen receptors as agonists. Similarly, the antagonistic activity of the derivatives was compared with tamoxifen and flutamide in the presence of estradiol and dihydrotestosterone, respectively. Tamoxifen and flutamide significantly decreased FI at concentrations of 10 μM and 100 nM, respectively. Again, no change in FI was observed for the tested derivatives at 10 μM.

Using a commercially available dual estrogen receptor TR-FRET assay for simultaneous measurement of steroid-site binding, modulation of estrogen receptor alpha and beta (ERα and ERβ) activity was evaluated using estriol and ICI182780 as comparators, with IC_{50} values below 3.31 nM and 5.12 nM, respectively. For the progesterone receptor (PR), progesterone and mifepristone were used as comparators, with IC_{50} values of 3.25 nM and 1.56 nM, respectively. Since none of the tested derivatives showed measurable activity even at 10 μM, their activity as endocrine disruptors can be ruled out.

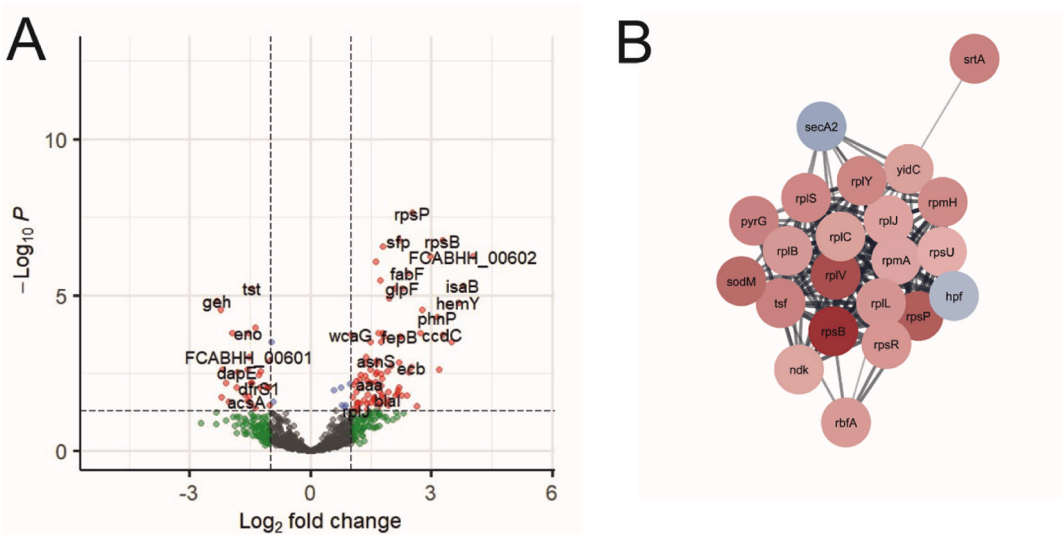

Fig. 11. Effect of erythromycin on *S. aureus* SA4 transcriptome. *(A)* Volcano plot - the red dots represent significantly up- and downregulated genes ($|\log2\ FC| \geq 1$ and $p < 0.05$). *(B)* Cytoscape network visualization of the nodes that represent genes, and the edges that represent links between genes. Red represents upregulated genes, and blue represents downregulated genes. (For interpretation of the references to colour in this figure legend, the reader is referred to the Web version of this article.)

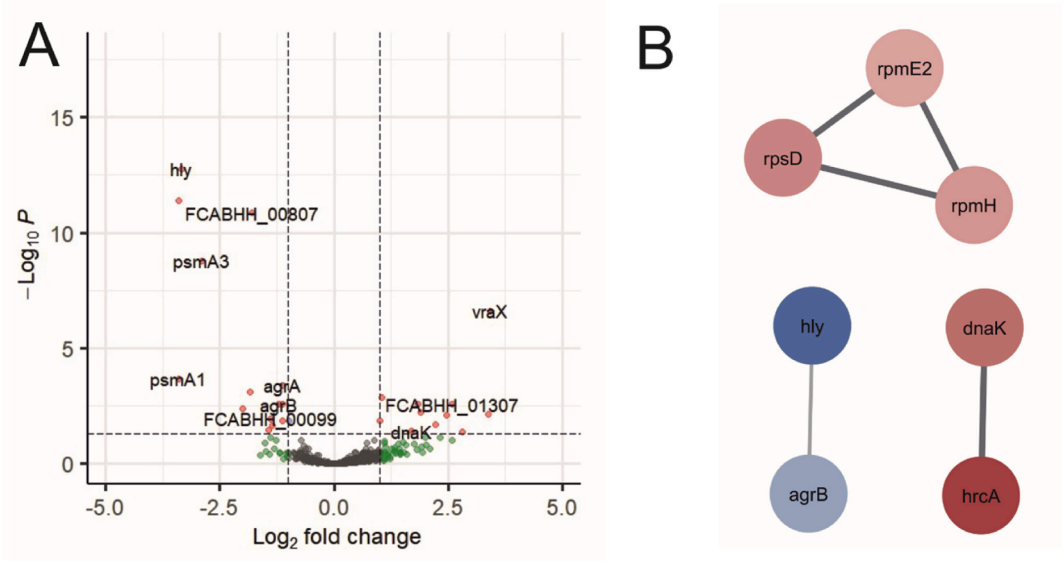

Fig. 12. Effect of derivative **13** on *S. aureus* SA4 transcriptome. *(A)* Volcano plot - the red dots represent significantly up- and downregulated genes ($|\log2\ FC| \geq 1$ and $p < 0.05$). *(B)* Cytoscape network visualization of the nodes that represent genes, and the edges that represent links between genes. Red represents upregulated genes, and blue represents downregulated genes. (For interpretation of the references to colour in this figure legend, the reader is referred to the Web version of this article.)

3.10. Computational analysis of compound 13 - LmrS interactions

To elucidate the potential molecular interactions between the most active steroidal compound and bacterial efflux pump LmrS, a series of computational analyses were performed. These included prediction of the efflux antiporter's three-dimensional structure, identification of possible ligand-binding sites, refinement of ligand poses by docking, and molecular dynamics (MD) simulations to assess complex stability. Each step provided a set of hypotheses rather than definitive conclusions, given the computational limitations and the inherent flexibility of the transporter.

All algorithms produced plausible structures consistent with the expected topology and function of major facilitator superfamily (MFS) transporters. However, most methods predicted only an outward-open conformation, whereas functional antiporters undergo large scale conformational changes between outward- and inward-open states. Notably, Boltz 2 yielded two distinct conformational clusters corresponding to these states with minimal structural variability within each cluster (Fig. 14). The Boltz 2 models were thus selected for further analyses as the most representative of the transporter's conformational range.

AlphaFold 3 and DiffDock consistently located potential binding pockets within the transmembrane channel region, while Boltz 2 predicted binding near the extracellular vestibule. These results collectively suggested that the steroid derivative may interact either within the substrate translocation pathway or at its extracellular entrance, potentially modulating efflux efficiency. Since AI-based binding predictions are approximate, we refined the ligand poses using conventional

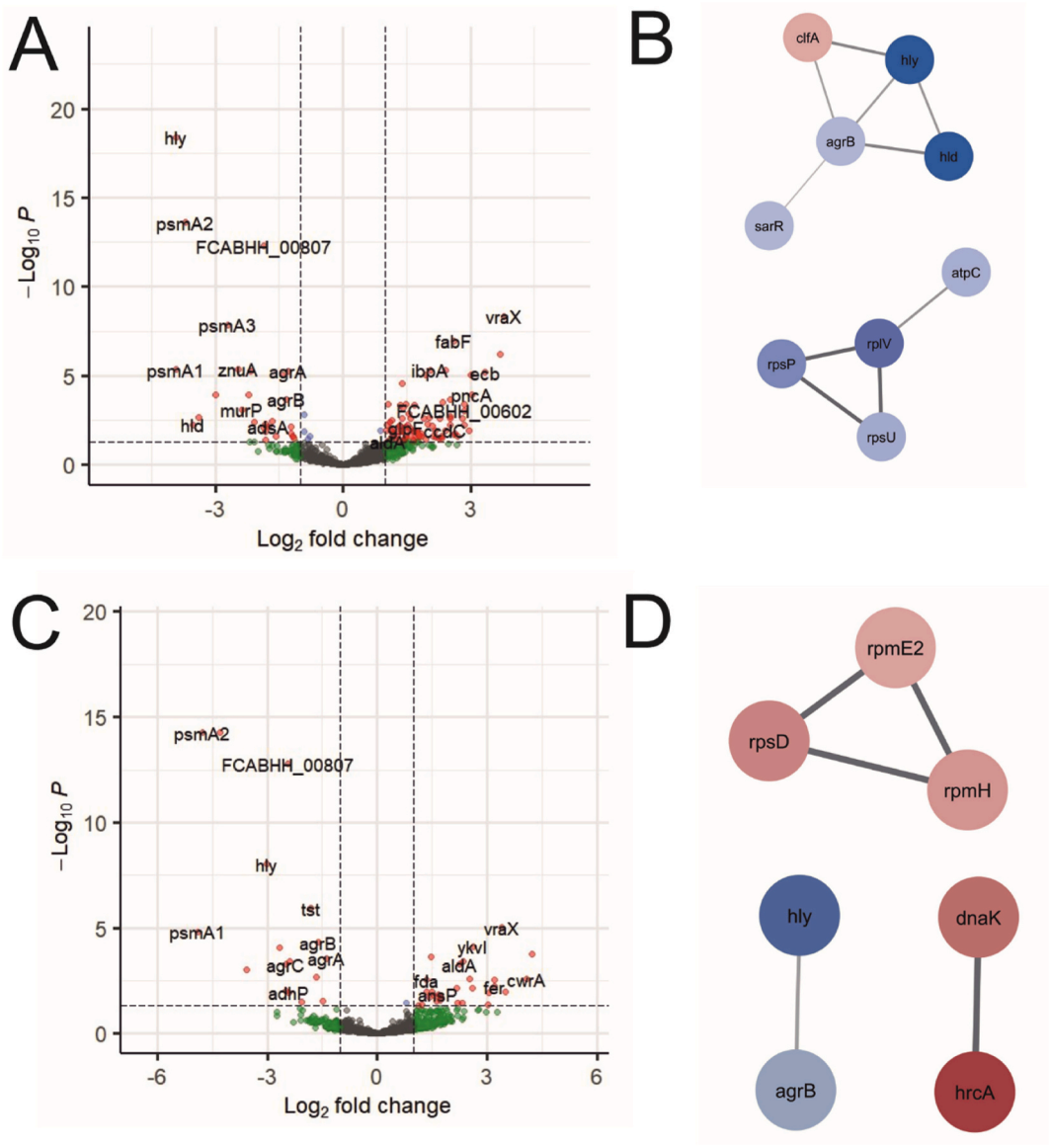

Fig. 13. Effect of compound **13** in combination with erythromycin *(A, B)* or ciprofloxacin *(C, D)* on *S. aureus* SA4 transcriptome. (*A, C)* Volcano plot - the red dots represent significantly up- and downregulated genes ($|\log2\ FC| \geq 1$ and $p < 0.05$). (*B, D)* Cytoscape network visualization of the nodes that represent genes, and the edges that represent links between genes. Red represents upregulated genes, and blue represents downregulated genes. (For interpretation of the references to colour in this figure legend, the reader is referred to the Web version of this article.)

Table 3
Minimum inhibitory concentrations (MIC) of selected steroidal compounds with the highest antibacterial activity, tested against three multidrug-resistant *S. aureus* strains (SA4, M334, and M53). Data are presented as the average of three replicates ± standard error of the mean (SEM).

MIC [μM]			
Compound	SA4	M334	M53
14	9.00 ± 0.58	12.88 ± 0.28	13.50 ± 0.41
15	11.00 ± 0.50	25.75 ± 0.61	13.13 ± 1.25
24	18.50 ± 0.76	17.67 ± 1.16	21.33 ± 1.20
25	17.50 ± 0.58	18.42 ± 1.56	21.17 ± 0.67
26	20.17 ± 1.48	27.25 ± 0.61	19.82 ± 0.17

For concentrations in μg/mL, see Supplementary Table S20–S21.

molecular docking with AutoDock Vina. The predicted AI-derived pockets served as initial search regions. The docking simulations revealed several energetically favorable orientations of the steroid scaffold compatible with hydrophobic and hydrogen-bonding interactions involving residues lining the transport channel. These results support a plausible binding mode consistent with the proposed inhibitory mechanism.

To further assess the stability of the predicted ligand-antiporter complexes, we performed all-atom molecular dynamics simulations (100 ns) using OpenMM. Each simulation system included the transporter embedded in an explicit aqueous environment with counterions and the docked steroid molecule. The trajectories confirmed that the most favorable ligand conformations remained stably bound throughout the simulation, with transient but recurrent interactions between the steroid and residues at the inner cavity and vestibular regions (Figs. 15–17). These observations suggest that the steroid derivative could transiently obstruct the transport pathway, consistent with an efflux inhibition mechanism.

While the presented analysis used substantial computing resources (hundreds of hours of GPU time), it still remains very approximate at best. The main source of uncertainty is the long-range movement of the

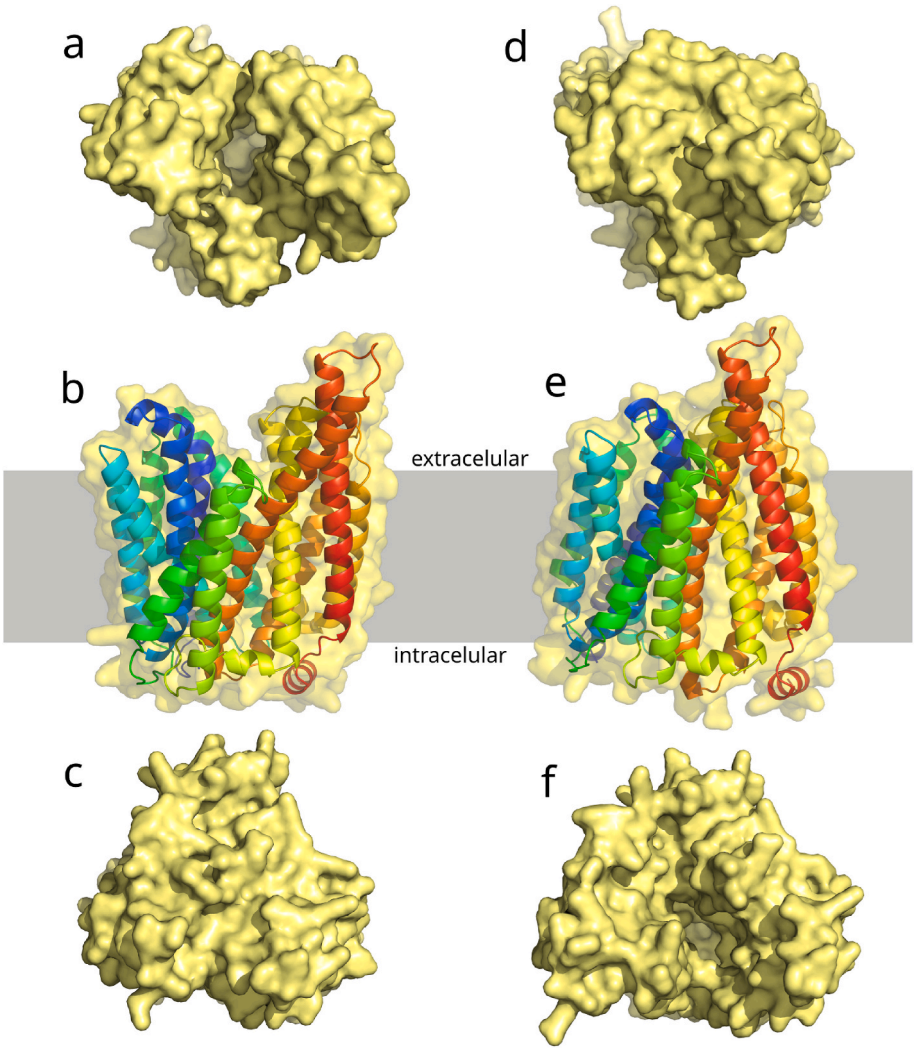

Fig. 14. Predicted conformations of the efflux antiporter by Boltz 2. *(A,B,C)* outward-open state, *(D,E,F)* inward-open state. Looking at the cell from the outside is depicted in *(A,D)*; from the inside on *(C,F)*. View alongside the cell membrane is at *(B,E)*. Protein's N-terminal is blue, C-terminal is red. (For interpretation of the references to colour in this figure legend, the reader is referred to the Web version of this article.)

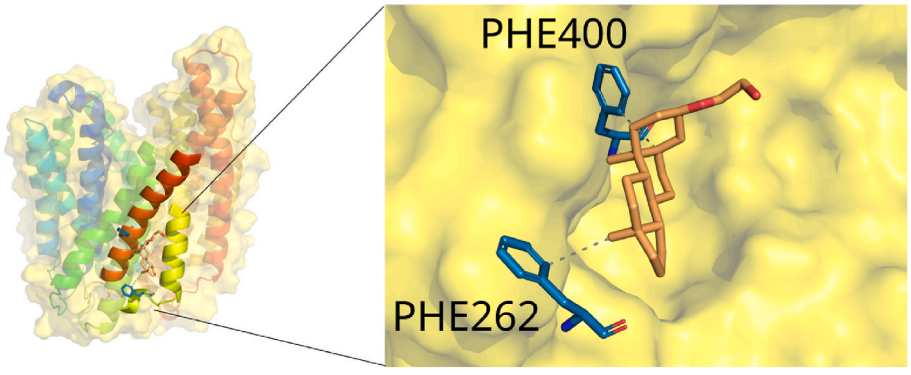

Fig. 15. One of the predicted steroid-binding poses touching the membrane. Stability in this well shaped hydrophobic pocket looks high, however blocking the transporter function would require strong allosteric effect.

protein. Prediction of two very distinct states is a notable success of Boltz 2, however all the intermediate states of the transition between extreme states should be explored for docking possibilities as well. This would likely require a complex (and maybe novel) combination of multiple protein structure prediction tools.

4. Conclusion

The aim of this study was to verify the hypothesis that endogenous steroid hormones, neurosteroids, and their synthetic analogues influence the activity of bacterial efflux pumps and are thus capable of increasing the efficacy of antibiotics. To assess their activity, two

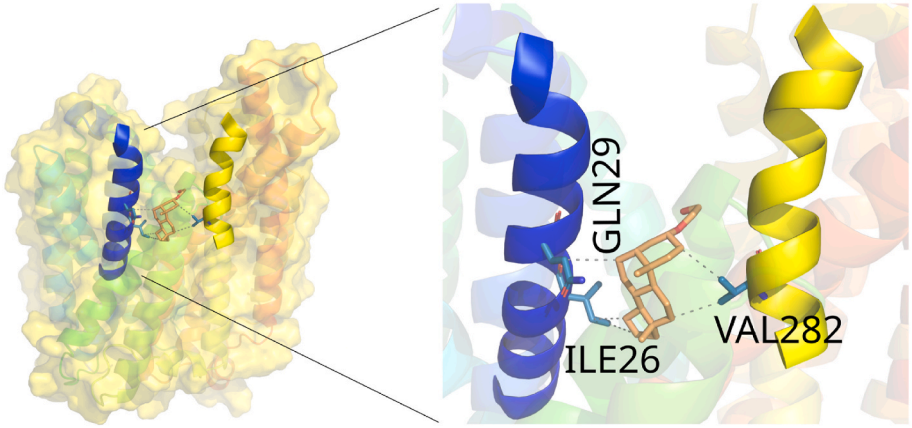

Fig. 16. Predicted steroid-binding pose in the channel. There are multiple other very close mostly hydrophobic binding sites. Molecular dynamics show strong propensity of the ligand to stay at one of these places or travel among them. Binding seems mostly hydrophobic with polar ligand tail sometimes intermittently binding various places.

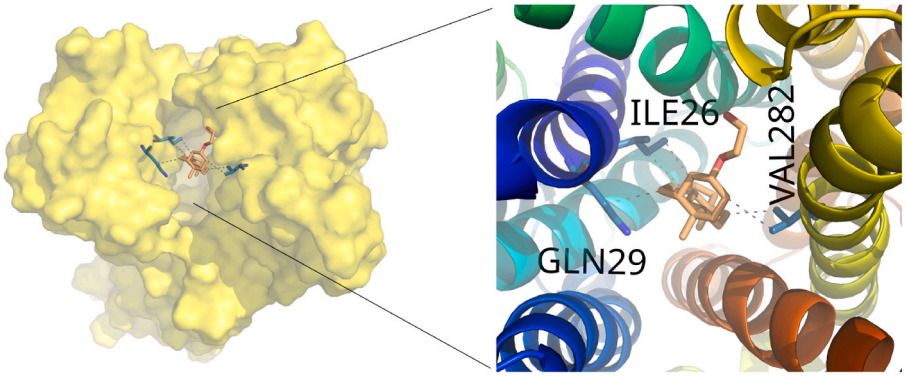

Fig. 17. Predicted steroid-binding pose in the channel, as seen from the extracellular space.

complementary assays were performed: an EtBr accumulation assay for direct efflux measurement, and an antibiotic sensitization assay (with ciprofloxacin or erythromycin) for functional MIC reduction. We demonstrated that certain endogenous steroid hormones and neurosteroids possess measurable, though limited, efflux pump inhibitory activity in multidrug-resistant *Staphylococcus aureus*. Pregnanolone, identified as the most active endogenous compound, was selected as the scaffold for the design and synthesis of novel derivatives with markedly improved potency. The subsequent SAR study identified compounds **13** and **16** as lead structures, combining strong inhibition under ciprofloxacin- and erythromycin-induced conditions with significant MIC reduction. Synthetic modifications affording compounds **13** and **16** demonstrated that the 3α,5β-stereochemistry, which defines the bent steroidal skeleton, is preferable. Polar, endogenous substitutions of the *D*-ring at position C-17 proved suboptimal, whereas nonpolar modifications such as exomethylene or ethylidene were favored. The most promising synthetic modification at position C-17 was the removal of all substituents. In contrast, the C-3 hydroxyl group requires polar modifications to achieve strong efflux pump inhibition and low MIC values in combination with ciprofloxacin. Such polar modifications can be introduced through hemiester substituents, tolerating hemimalonate, hemisuccinate, and hemiglutarate moieties. Additionally, polar modifications at position C-3 can be achieved *via* an ethylene glycol linker further derivatized at the secondary hydroxyl group, for example, with L-pyroglutamic acid or 6-oxopiperidine acid. Finally, we demonstrated that modifications at positions C-3 and C-17 are crucial for potent efflux pump inhibition and sensitization to ciprofloxacin, yet their effects are not additive. Checkerboard assays confirmed additive interactions when combined with antibiotics. Transcriptomic profiling of compound **13** revealed substantial transcriptional reprogramming, including marked downregulation of multiple stress- and virulence-associated genes when administered alone or in combination with ciprofloxacin and erythromycin, indicating an additional anti-virulence effect. Importantly, the most active derivatives were non-cytotoxic and lacked measurable endocrine activity, underscoring their potential as safe and effective antibiotic adjuvants. Given that efflux pump systems contribute not only to multidrug resistance but also to bacterial virulence, their inhibition represents a promising approach for restoring antibiotic efficacy. These findings highlight the promise of rationally designed androstane-based scaffolds as a means to overcome efflux-mediated resistance and enhance the clinical utility of existing antibiotics.

Declaration of generative AI and AI-assisted technologies in the writing process

During the preparation of this work, the authors (EK, DB) used ChatGPT to improve the language quality of the manuscript, as they are not native English speakers. After using this tool/service, the author reviewed and edited the content as needed and takes full responsibility for the content of the publication.

Funding resources

This work was supported by the Technology Agency of the Czech Republic, National Center of Competence – Personalized Medicine: From Translational Research into Biomedical Applications

(TN02000109) and by the project National Institute of Virology and Bacteriology (Programme EXCELES, ID Project No. LX22NPO5103) - Funded by the European Union - Next Generation EU. This work was supported by the Academy of Sciences of the Czech Republic grant RVO 61388963, by the Ministry of Health of the Czech Republic in cooperation with the Czech Health Research Council under project No. NU23-09-00080, and by the Ministry of Education, Youth and Sports of the Czech Republic grant for Talking Microbes – understanding microbial interactions within the One Health framework (grant no. CZ.02.01.01/00/22_008/0004597), and LUC24099. This publication is partly based upon work from COST Action EURESTOP, CA21145, supported by COST (European Cooperation in Science and Technology). Computing resources for ligand position analysis were provided by ELIXIR CZ (LM2023055).

CRediT authorship contribution statement

Daniela Brdová: Data curation, Formal analysis, Investigation, Methodology, Writing – original draft, Writing – review & editing. **Bára Křížkovská:** Investigation, Methodology, Writing – review & editing. **Jan Špaček:** Data curation, Investigation, Methodology, Software, Visualization. **Zdeněk Míchal:** Investigation, Writing – review & editing. **Eva Jablonská:** Investigation, Writing – review & editing. **Ondřej Strnad:** Investigation, Methodology, Writing – review & editing. **Hana Chodounská:** Investigation. **Eszter Szánti-Pintér:** Investigation. **Marina Morozovová:** Investigation. **Václav Hanžl:** Investigation. **Jan Tkadlec:** Investigation, Writing – review & editing. **Martijn Riool:** Methodology, Writing – review & editing. **Jan Lipov:** Investigation, Writing – review & editing. **Jitka Viktorová:** Conceptualization, Formal analysis, Funding acquisition, Methodology, Project administration, Supervision, Validation, Visualization, Writing – original draft, Writing – review & editing. **Eva Kudová:** Conceptualization, Funding acquisition, Project administration, Supervision, Writing – original draft, Writing – review & editing.

Declaration of competing interest

The authors declare the following financial interests/personal relationships which may be considered as potential competing interests: Eva Kudova, Jitka Viktorova reports financial support was provided by Technology Agency of the Czech Republic. Jan Tkadlec reports financial support was provided by Ministry of Health of the Czech Republic. Jitka Viktorova reports financial support was provided by Ministry of Education, Youth and Sports of the Czech Republic grant for Talking Microbes. Vaclav Hanzl reports financial support was provided by ELIXIR CZ. If there are other authors, they declare that they have no known competing financial interests or personal relationships that could have appeared to influence the work reported in this paper.

Appendix A. Supplementary data

Supplementary data to this article can be found online at https://doi.org/10.1016/j.ejmech.2026.118716.

Data availability

Data are included in Supplements and also have been submitted to the BioSample database (NCBI).

References

[1] H. Ozawa, Steroid hormones, their receptors and neuroendocrine system, J. Nippon Med. Sch. 72 (2005) 316–325.
[2] S. Bairamova, D. Petelin, A. Vitalievich, N. Kudryashov, O. Sorokina, S. Semin, V. Panfilova, B. Volel, The endogenic neurosteroid system and its role in the pathogenesis and therapy of mental disorders, Research Results in Pharmacology 9 (2023) 61–69.
[3] S.R. Wilkenfeld, C. Lin, D.E. Frigo, Communication between genomic and non-genomic signaling events coordinate steroid hormone actions, Steroids 133 (2018) 2–7.
[4] E. Lloyd-Evans, H. Waller-Evans, Biosynthesis and signalling functions of central and peripheral nervous system neurosteroids in health and disease, Essays Biochem. 64 (2020) 591–606.
[5] D. Adhya, E. Annuario, M.A. Lancaster, J. Price, S. Baron-Cohen, D.P. Srivastava, Understanding the role of steroids in typical and atypical brain development: advantages of using a "brain in a dish" approach, J. Neuroendocrinol. 30 (2018) e12547.
[6] V. Nisenblat, B. Engel-Yeger, G. Ohel, D. Aronson, M. Granot, The association between supra-physiological levels of estradiol and response patterns to experimental pain, Eur. J. Pain 14 (2010) 840–846.
[7] T. Iqbal, A. Elahi, W. Wijns, A. Shahzad, Cortisol detection methods for stress monitoring in connected health, Health Sciences Review 6 (2023) 100079.
[8] V. Hána, J. Ježková, M. Kosák, M. Kršek, V. Hána, M. Hill, Serum steroid profiling in Cushing's syndrome patients, J. Steroid Biochem. Mol. Biol. 192 (2019) 105410.
[9] M. Hill, A. Pašková, R. Kančeva, M. Velíková, J. Kubátová, L. Kancheva, K. Adamcová, M. Mikešová, Z. Žižka, M. Koucký, H. Šarapatková, V. Kačer, P. Matucha, M. Meloun, A. Parízek, Steroid profiling in pregnancy: a focus on the human fetus, J. Steroid Biochem. Mol. Biol. 139 (2014) 201–222.
[10] S. Luisi, F. Petraglia, C. Benedetto, R.E. Nappi, F. Bernardi, M. Fadalti, F.M. Reis, M. Luisi, A.R. Genazzani, Serum allopregnanolone levels in pregnant women: changes during pregnancy, at delivery, and in hypertensive patients, J. Clin. Endocrinol. Metab. 85 (2000) 2429–2433.
[11] M. Hill, A. Parízek, R. Kancheva, J.E. Jirásek, Reduced progesterone metabolites in human late pregnancy, Physiol. Res. 60 (2011) 225–241.
[12] M. Hill, V. Hána Jr., M. Velíková, A. Parízek, L. Kolátorová, J. Vítků, T. Škodová, M. Šimková, P. Šimják, R. Kancheva, M. Koucký, Z. Kokrdová, K. Adamcová, A. Černý, Z. Hájek, M. Dušková, J. Bulant, L. Stárka, A method for determination of one hundred endogenous steroids in human serum by gas chromatography-tandem mass spectrometry, Physiol. Res. 68 (2019) 179–207.
[13] S. Sam, T.C. Corbridge, B. Mokhlesi, A.P. Comellas, M.E. Molitch, Cortisol levels and mortality in severe sepsis, Clin. Endocrinol. 60 (2004) 29–35.
[14] R.H.K. Emanuel, J. Roberts, P.D. Docherty, H. Lunt, R.E. Campbell, K. Möller, A review of the hormones involved in the endocrine dysfunctions of polycystic ovary syndrome and their interactions, Front. Endocrinol. 13 (2022) 1017468.
[15] M. Patt, L. Conte, M. Blaha, B. Plotkin, Steroid hormones as interkingdom signaling molecules: innate immune function and microbial colonization modulation, AIMS Molecular Science 5 (2018) 117–130.
[16] F. Kalaycı-Yüksek, D. Gümüş, V. Güler, A. Uyanık-Öcal, M. Anğ-Küçüker, Progesterone and estradiol alter the growth, virulence and antibiotic susceptibilities of *Staphylococcus aureus*, New Microbiol. 46 (2023) 43–51.
[17] Z. Luo, H. Xi, W. Huang, M.F. Liu, L. Yuan, Q. Chen, Y. Xiao, Q. Zhu, R. Zhao, Y. Y. Sheng, The role of male hormones in bacterial infections: enhancing *Staphylococcus aureus* virulence through testosterone-induced Agr activation, Arch. Microbiol. 206 (2024) 401.
[18] A. Vollaro, A. Esposito, E. Antonaki, V.D. Iula, D. D'Alonzo, A. Guaragna, E. De Gregorio, Steroid derivatives as potential antimicrobial agents against *Staphylococcus aureus* planktonic cells, Microorganisms 8 (2020) 468.
[19] E.R. Vázquez-Martínez, E. García-Gómez, I. Camacho-Arroyo, B. González-Pedrajo, Sexual dimorphism in bacterial infections, Biol. Sex Differ. 9 (2018) 27.
[20] E. García-Gómez, B. González-Pedrajo, I. Camacho-Arroyo, Role of sex steroid hormones in bacterial-host interactions, BioMed Res. Int. 2013 (2013) 928290.
[21] B. Plotkin, R. Roose, Q. Erikson, S. Viselli, Effect of androgens and glucocorticoids on microbial growth and antimicrobial susceptibility, Curr. Microbiol. 47 (2004) 514–520.
[22] D. Brdová, T. Ruml, J. Viktorová, Mechanism of staphylococcal resistance to clinically relevant antibiotics, Drug Resist. Updates 77 (2024) 101147.
[23] R. Mineiro, C. Santos, I. Gonçalves, M. Lemos, J.E.B. Cavaco, T. Quintela, Regulation of ABC transporters by sex steroids may explain differences in drug resistance between sexes, J. Physiol. Biochem. 79 (2023) 467–487.
[24] C.A. Elkins, L.B. Mullis, Mammalian steroid hormones are substrates for the major RND- and MFS-type tripartite multidrug efflux pumps of Escherichia coli, J. Bacteriol. 188 (2006) 1191–1195.
[25] A. Luqman, The orchestra of human bacteriome by hormones, Microb. Pathog. 180 (2023) 106125.
[26] E. Stastna, H. Chodounska, V. Pouzar, V. Kapras, J. Borovska, O. Cais, L. Vyklicky Jr., Synthesis of C3, C5, and C7 pregnane derivatives and their effect on NMDA receptor responses in cultured rat hippocampal neurons, Steroids 74 (2009) 256–263.
[27] H. Chodounska, V. Kapras, L. Vyklicky, J. Borovska, V. Vyklicky, K. Vales, Compounds for Treatment of Neurodegenerative and Neuropsychiatric Disorders, 2013. US201333838, in: US2013338383A1.
[28] J. Borovska, V. Vyklicky, E. Stastna, V. Kapras, B. Slavikova, M. Horak, H. Chodounska, L. Vyklicky Jr., Access of inhibitory neurosteroids to the NMDA receptor, Br. J. Pharmacol. 166 (2012) 1069–1083.
[29] E. Kudova, H. Chodounska, P. Mares, K. Vales, 3Alpha, 5Beta-Neuroactive Steroids for the Treatment of Epilepsy and Seizure Diseases, 2023. CA3128921(C).
[30] E. Kudova, H. Chodounska, B. Slavikova, M. Budesinsky, M. Nekardova, V. Vyklicky, B. Krausova, P. Svehla, L. Vyklicky, A new class of potent *N*-Methyl-*D*-Aspartate receptor inhibitors: sulfated neuroactive steroids with lipophilic *D*-Ring modifications, J. Med. Chem. 58 (2015) 5950–5966.
[31] B. Slavikova, J. Bujons, L. Matyas, M. Vidal, Z. Babot, Z. Kristofikova, C. Sunol, A. Kasal, Allopregnanolone and pregnanolone analogues modified in the *C* ring: synthesis and activity, J. Med. Chem. 56 (2013) 2323–2336.

[32] E. Kudova, H. Chodounska, V. Kapras, L. Vyklicky, K. Vales, U. Jahn, Amphiphilic Compounds with Neuroprotective Properties, 2018. US 10,017,535 B2, 2018.
[33] B. Krausova, B. Slavikova, M. Nekardova, P. Hubalkova, V. Vyklicky, H. Chodounska, L. Vyklicky, E. Kudova, Positive modulators of the *N*-Methyl-*D*-aspartate receptor: Structure-activity relationship study of steroidal 3-Hemiesters, J. Med. Chem. 61 (2018) 4505–4516.
[34] C.E. Weaver, M.B. Land, R.H. Purdy, K.G. Richards, T.T. Gibbs, D.H. Farb, Geometry and charge determine pharmacological effects of steroids on *N*-Methyl-*D*-aspartate receptor-induced Ca2+ accumulation and cell death, J. Pharmacol. Exp. Therapeut. 293 (2000) 747–754.
[35] M. Hanzlova, B. Slavikova, M. Morozovova, K. Musilek, A. Rotterova, L. Zemanová, E. Kudova, C-3 steroidal hemiesters as inhibitors of 17β-Hydroxysteroid dehydrogenase type 10, ACS Omega 9 (2024) 12116–12124.
[36] B. Křížkovská, L. Hoang, D. Brdová, K. Klementová, N. Szemerédi, A. Loučková, O. Kronusová, G. Spengler, P. Kaštánek, J. Hajšlová, J. Viktorová, J. Lipov, Modulation of the bacterial virulence and resistance by well-known European medicinal herbs, J. Ethnopharmacol. 312 (2023) 116484.
[37] K. Holasová, B. Křížkovská, L. Hoang, S. Dobiasová, J. Lipov, T. Macek, V. Křen, K. Valentová, T. Ruml, J. Viktorová, Flavonolignans from silymarin modulate antibiotic resistance and virulence in *Staphylococcus aureus*, Biomed. Pharmacother. 149 (2022) 112806.
[38] N. Fatsis-Kavalopoulos, D.L. Sánchez-Hevia, D.I. Andersson, Beyond the FIC index: the extended information from fractional inhibitory concentrations (FICs), J. Antimicrob. Chemother. 79 (2024) 2394–2396.
[39] EPA, Endocrine Disruptor Screening Program Test Guidelines – OPPTS 890.1300: Estrogen Receptor Transcriptional Activation (Human Cell Line (HeLa-9903)); EPA 740-C-09-006, U.S. Environmental Protection Agency, Washington, DC, 2009.
[40] OECD, Test No. 455: Performance-Based Test Guideline for Stably Transfected Transactivation *in Vitro* Assays to Detect Estrogen Receptor Agonists and Antagonists, OECD Publishing, Paris, 2021, 2021.
[41] V.S. Wilson, K. Bobseine, C.R. Lambright, L.E. Gray Jr., A novel cell line, MDA-kb2, that stably expresses an androgen- and glucocorticoid-responsive reporter for the detection of hormone receptor agonists and antagonists, Toxicol. Sci. 66 (2002) 69–81.
[42] OECD, Test No. 458: Stably Transfected Human Androgen Receptor Transcriptional Activation Assay for Detection of Androgenic Agonist and Antagonist Activity of Chemicals; OECD Guidelines for the Testing of Chemicals, Section 4, OECD Publishing, Paris, 2023, 2023.
[43] F. Grünberger, S. Ferreira-Cerca, D. Grohmann, Nanopore sequencing of RNA and cDNA molecules in Escherichia coli, Rna 28 (2022) 400–417.
[44] R. Patro, G. Duggal, M.I. Love, R.A. Irizarry, C. Kingsford, Salmon: fast and bias-aware quantification of transcript expression using dual-phase inference, Nat. methods 14 (2017) 417–419. Article number: 28263959.
[45] M. Kolmogorov, J. Yuan, Y. Lin, P.A. Pevzner, Assembly of long, error-prone reads using repeat graphs, Nat. Biotechnol. 37 (2019) 540–546.
[46] O. Schwengers, L. Jelonek, M.A. Dieckmann, S. Beyvers, J. Blom, A. Goesmann, Bakta: rapid and standardized annotation of bacterial genomes *via* alignment-free sequence identification, Microb. Genom. 7 (2021).
[47] S. Passaro, G. Corso, J. Wohlwend, M. Reveiz, S. Thaler, V.R. Somnath, N. Getz, T. Portnoi, J. Roy, H. Stark, D. Kwabi-Addo, D. Beaini, T. Jaakkola, R. Barzilay, Boltz-2: towards accurate and efficient binding affinity prediction, bioRxiv (2025), https://doi.org/10.1101/2025.06.14.659707.
[48] O. Trott, A.J. Olson, AutoDock vina: improving the speed and accuracy of docking with a new scoring function, efficient optimization, and multithreading, J. Comput. Chem. 31 (2010) 455–461.
[49] P. Eastman, J. Swails, J.D. Chodera, R.T. McGibbon, Y. Zhao, K.A. Beauchamp, L. P. Wang, A.C. Simmonett, M.P. Harrigan, C.D. Stern, R.P. Wiewiora, B.R. Brooks, V.S. Pande, OpenMM 7: rapid development of high performance algorithms for molecular dynamics, PLoS Comput. Biol. 13 (2017) e1005659.
[50] A. Dashtbani-Roozbehani, M.H. Brown, Efflux pump mediated antimicrobial resistance by staphylococci in health-related environments: challenges and the quest for inhibition, Antibiotics 10 (2021) 1502.
[51] S. Sinha, S. Aggarwal, D.V. Singh, Efflux pumps: gatekeepers of antibiotic resistance in *Staphylococcus aureus* biofilms, Microb. Cell 11 (2024) 368–377.
[52] S.S. Costa, M. Viveiros, L. Amaral, I. Couto, Multidrug efflux pumps in *staphylococcus aureus*: an update, Open Microbiol. J. 7 (2013) 59–71.
[53] S. Kumar, M.F. Varela, Biochemistry of bacterial multidrug efflux pumps, Int. J. Mol. Sci. 13 (2012) 4484–4495.
[54] S. Hassanzadeh, R. Mashhadi, M. Yousefi, E. Askari, M. Saniei, M.R. Pourmand, Frequency of efflux pump genes mediating ciprofloxacin and antiseptic resistance in methicillin-resistant *Staphylococcus aureus* isolates, Microb. Pathog. 111 (2017) 71–74.
[55] G.D. Anderson, P.S. Odegard, Pharmacokinetics of estrogen and progesterone in chronic kidney disease, Adv Chronic Kidney Dis 11 (2004) 357–360.
[56] M. Hill, D. Cibula, H. Havlikova, L. Kancheva, T. Fait, R. Kancheva, A. Parizek, L. Starka, Circulating levels of pregnanolone isomers during the third trimester of human pregnancy, J. Steroid Biochem. Mol. Biol. 105 (2007) 166–175.
[57] Y. Jin, A.C. Mesaros, I.A. Blair, T.M. Penning, Stereospecific reduction of 5beta-reduced steroids by human ketosteroid reductases of the AKR (aldo-keto reductase) superfamily: role of AKR1C1-AKR1C4 in the metabolism of testosterone and progesterone *via* the 5beta-reductase pathway, Biochem. J. 437 (2011) 53–61.
[58] Y.V. Wu, W.M. Burnham, Progesterone, 5a-dihydropogesterone and allopregnanolone's effects on seizures: a review of animal and clinical studies, Seizure 63 (2018) 26–36.
[59] M. Chen, T.M. Penning, 5beta-Reduced steroids and human Delta(4)-3-ketosteroid 5beta-reductase (AKR1D1), Steroids 83 (2014) 17–26.
[60] J.W. Jonker, C. Liddle, M. Downes, FXR and PXR: potential therapeutic targets in cholestasis, J. Steroid Biochem. Mol. Biol. 130 (2012) 147–158.
[61] E. Kudova, Rapid effects of neurosteroids on neuronal plasticity and their physiological and pathological implications, Neurosci. Lett. 750 (2021) 135771.
[62] R. Thänert, O. Goldmann, A. Beineke, E. Medina, Host-inherent variability influences the transcriptional response of *Staphylococcus aureus* during *in vivo* infection, Nat. Commun. 8 (2017) 14268.
[63] J. Yan, D. Han, C. Liu, Y. Gao, D. Li, Y. Liu, G. Yang, *Staphylococcus aureus* VraX specifically inhibits the classical pathway of complement by binding to C1q, Mol. Immunol. 88 (2017) 38–44.
[64] Y. Lu, F. Chen, Q. Zhao, Q. Cao, R. Chen, H. Pan, Y. Wang, H. Huang, R. Huang, Q. Liu, M. Li, T. Bae, H. Liang, L. Lan, Modulation of MRSA virulence gene expression by the wall teichoic acid enzyme TarO, Nat. Commun. 14 (2023) 1594.
[65] M.R. Guna Serrano, N. Larrosa Escartín, M. Marín Arriaza, J.C. Rodríguez Díaz, Microbiological diagnosis of bacteraemia and fungaemia: blood cultures and molecular methods, Enferm. Infecc. Microbiol. Clín. 37 (2019) 335–340.